OPEN ACCESS

ORIGINAL ARTICLE

Caffeine protects against experimental acute pancreatitis by inhibition of inositol 1,4,5-trisphosphate receptor-mediated Ca^{2+} release

Wei Huang,[1,2,3] Matthew C Cane,[2] Rajarshi Mukherjee,[1,2] Peter Szatmary,[1,2] Xiaoying Zhang,[1,3] Victoria Elliott,[1] Yulin Ouyang,[1,2] Michael Chvanov,[1,2] Diane Latawiec,[1] Li Wen,[1,3] David M Booth,[2] Andrea C Haynes,[4] Ole H Petersen,[5] Alexei V Tepikin,[2] David N Criddle,[1,2] Robert Sutton[1]

▶ Additional material is published online only. To view please visit the journal online (http://dx.doi.org/10.1136/gutjnl-2015-309363).

[1]NIHR Liverpool Pancreas Biomedical Research Unit, Royal Liverpool University Hospital, University of Liverpool, Liverpool, UK
[2]Department of Cellular and Molecular Physiology, Institute of Translational Medicine, University of Liverpool, Liverpool, UK
[3]Department of Integrated Traditional Chinese and Western Medicine, Sichuan Provincial Pancreatitis Centre, West China Hospital, Sichuan University, Chengdu, China
[4]Immuno-Inflammation Therapeutic Area Unit, GlaxoSmithKline, Stevenage, UK
[5]Cardiff School of Biosciences, Cardiff University, Cardiff, UK

Correspondence to
Professor Robert Sutton, NIHR Liverpool Pancreas Biomedical Research Unit, 5th Floor UCD, Royal Liverpool University Hospital, Daulby Street, Liverpool L69 3GA, UK; r.sutton@liverpool.ac.uk

Received 10 February 2015
Revised 31 August 2015
Accepted 22 September 2015
Published Online First 7 December 2015

To cite: Huang W, Cane MC, Mukherjee R, *et al*. *Gut* 2017;**66**:301–313.

ABSTRACT

Objective Caffeine reduces toxic Ca^{2+} signals in pancreatic acinar cells via inhibition of inositol 1,4,5-trisphosphate receptor (IP_3R)-mediated signalling, but effects of other xanthines have not been evaluated, nor effects of xanthines on experimental acute pancreatitis (AP). We have determined effects of caffeine and its xanthine metabolites on pancreatic acinar IP_3R-mediated Ca^{2+} signalling and experimental AP.

Design Isolated pancreatic acinar cells were exposed to secretagogues, uncaged IP_3 or toxins that induce AP and effects of xanthines, non-xanthine phosphodiesterase (PDE) inhibitors and cyclic adenosine monophosphate and cyclic guanosine monophosphate (cAMP/cGMP) determined. The intracellular cytosolic calcium concentration ($[Ca^{2+}]_C$), mitochondrial depolarisation and necrosis were assessed by confocal microscopy. Effects of xanthines were evaluated in caerulein-induced AP (CER-AP), taurolithocholic acid 3-sulfate-induced AP (TLCS-AP) or palmitoleic acid plus ethanol-induced AP (fatty acid ethyl ester AP (FAEE-AP)). Serum xanthines were measured by liquid chromatography-mass spectrometry.

Results Caffeine, dimethylxanthines and non-xanthine PDE inhibitors blocked IP_3-mediated Ca^{2+} oscillations, while monomethylxanthines had little effect. Caffeine and dimethylxanthines inhibited uncaged IP_3-induced Ca^{2+} rises, toxin-induced Ca^{2+} release, mitochondrial depolarisation and necrotic cell death pathway activation; cAMP/cGMP did not inhibit toxin-induced Ca^{2+} rises. Caffeine significantly ameliorated CER-AP with most effect at 25 mg/kg (seven injections hourly); paraxanthine or theophylline did not. Caffeine at 25 mg/kg significantly ameliorated TLCS-AP and FAEE-AP. Mean total serum levels of dimethylxanthines and trimethylxanthines peaked at >2 mM with 25 mg/kg caffeine but at <100 μM with 25 mg/kg paraxanthine or theophylline.

Conclusions Caffeine and its dimethylxanthine metabolites reduced pathological IP_3R-mediated pancreatic acinar Ca^{2+} signals but only caffeine ameliorated experimental AP. Caffeine is a suitable starting point for medicinal chemistry.

Significance of this study

What is already known on this subject?

- Acute pancreatitis is a major health problem without specific drug therapy.
- Coffee consumption reduces the incidence of acute alcoholic pancreatitis.
- Caffeine blocks physiological intracellular Ca^{2+} oscillations by inhibition of inositol 1,4,5-trisphosphate receptor-(IP_3R)-mediated signalling.
- Sustained cytosolic Ca^{2+} overload from abnormal Ca^{2+} signalling is implicated as a critical trigger in the pathogenesis of acute pancreatitis.

What are the new findings?

- Caffeine and its dimethylxanthine metabolites inhibit IP_3R-mediated, sustained cytosolic Ca^{2+} elevations, loss of mitochondrial membrane potential and necrotic cell death pathway activation in pancreatic acinar cells.
- Neither specific phosphodiesterase inhibitors nor cyclic adenosine monophosphate and cyclic guanosine monophosphate inhibit sustained Ca^{2+} elevations in pancreatic acinar cells.
- Serum levels of xanthines after 25 mg/kg caffeine administration are sufficient to inhibit IP_3R-mediated Ca^{2+} overload in experimental acute pancreatitis.
- Caffeine but not theophylline or paraxanthine administered at 25 mg/kg significantly ameliorated pancreatic injury in experimental acute pancreatitis through IP_3R-mediated signalling inhibition.

How might it impact on clinical practice in the foreseeable future?

- These findings support an approach of inhibition of Ca^{2+} overload and of its consequences as novel potential therapy for acute pancreatitis.
- Methylxanthine-based structures are suitable starting points for drug discovery and development to treat acute pancreatitis.

INTRODUCTION

Acute pancreatitis (AP) has an incidence of 30 per 100 000 per annum in the UK, commonly caused by gallstones or alcohol excess.[1] Most cases are

mild, whereas a complicated clinical course occurs in one out of every five patients, resulting in significant morbidity, mortality and financial burden.[2] Over the last two decades, our understanding of pathogenesis has advanced, but there is still no specific therapy despite many randomised trials.[2] The development of treatments for AP is, therefore, a priority, one strategy for which is to follow leads from complementary laboratory and clinical studies, as here.

Intracellular Ca^{2+} signals control normal secretion from pancreatic acinar cells but can become a critical trigger in pathogenesis. Physiological concentrations of acetylcholine (ACh) and cholecystokinin (CCK) generate repetitive elevations in the cytosolic Ca^{2+} concentration ($[Ca^{2+}]_C$) within the cellular apical pole that elicit stimulus metabolism coupling to generate ATP from mitochondria and stimulus-secretion coupling to initiate exocytosis.[3] Intermittently, global extension of short-lived signals throughout the cell is necessary for nuclear signalling contributing to transcription and translation.[3] In contrast, toxins such as bile acids,[4] oxidative[5] and non-oxidative metabolites[6 7] of ethanol and CCK hyperstimulation[8 9] each elicit abnormal elevations of $[Ca^{2+}]_C$ that are global and sustained. These abnormal elevations induce premature activation of intracellular enzymes, mitochondrial dysfunction, impaired autophagy, vacuolisation and necrosis, all of which contribute to the pathogenesis of AP.[10] Ca^{2+} chelation prevents zymogen activation and vacuolisation through attenuation of Ca^{2+} overload in acinar cells in vitro[11 12] and ameliorates the severity of AP in vivo.[13] Blockage of the Ca^{2+} release-activated Ca^{2+} channel, also known as the store-operated Ca^{2+} entry (SOCE) channel, by Orai1 inhibitor GSK-7975A, reduces Ca^{2+} overload and necrosis in both mouse[14 15] and human[15] pancreatic acinar cells and prevents AP in three different mouse models. Genetic deletion or pharmacological inhibition of another SOCE channel, transient receptor potential cation channel 3 (TRPC3), also reduces caerulein-induced SOCE and AP.[16 17]

Excessive Ca^{2+} release from intracellular stores occurs predominantly via inositol 1,4,5-trisphosphate receptor (IP_3R) Ca^{2+} channels.[18] The pancreatic acinar cell expresses all three subtypes of the IP_3R in the apical region, close to the luminal membrane,[19–21] but IP_3R types 2 and 3 are predominantly responsible for physiological Ca^{2+} signalling and enzyme secretion.[20] Stimuli such as CCK,[22] the bile acid taurolithocholic acid 3-sulfate (TLCS),[23 24] alcohol[25] and fatty acid ethyl ester (FAEE)[6 18] cause intracellular Ca^{2+} release in pancreatic acinar cells primarily via IP_3Rs, an effect inhibited by double knockout of IP_3R types 2 and 3[18] or by caffeine.[8 18]

Caffeine (1,3,7-trimethyxanthine) belongs to the methylxanthine class of small, purine-based planar molecules and has several pharmacological actions,[26] including pronounced actions on Ca^{2+} signalling.[27] Caffeine inhibits Ca^{2+} release from IP_3Rs by inhibition of phospholipase C-mediated production of IP_3[28] or by antagonising IP_3Rs[29] through direct binding and reduction of the open-state probability of IP_3Rs.[30 31] Contrarily, caffeine activates Ca^{2+} release from ryanodine receptors (RyRs) by increasing the sensitivity of RyRs to Ca^{2+} itself as observed in multiple cells,[32] although in pancreatic acinar cells effects on IP_3Rs predominate.[28 29]

The effects of caffeine on IP_3-mediated Ca^{2+} signalling may be protective in AP since the incidence of AP is inversely proportional to the amount of coffee consumed.[33] Caffeine also inhibits cyclic adenosine monophosphate (cAMP) and cyclic guanosine monophosphate (cGMP) phosphodiesterase (PDE), which degrades cAMP and cGMP to non-cyclic forms;[34] inhibition of PDE reduces tumour necrosis factor and leukotriene synthesis, inhibiting innate immunity.[35] Caffeine is a non-selective inhibitor of adenosine receptors, removing an endogenous brake on neural activity.[26] This stimulant effect of caffeine is the most familiar, but taken to excess may result in caffeine intoxication with major central nervous system hyperstimulation.[26] Degradation of caffeine in the liver forms the dimethylxanthines theophylline (1,3-dimethylxanthine), paraxanthine (1,7-dimethylxanthine) and theobromine (3,7-dimethylxanthine), used variously as drugs with similar actions to those of caffeine, although their actions on IP_3R-mediated signalling have not been clarified. As data suggest caffeine and/or related methylxanthines may be protective in AP, we sought to determine their actions on toxin-induced, IP_3R-mediated $[Ca^{2+}]_C$ changes and cell death in vitro, and in three models of AP in vivo.

MATERIALS AND METHODS

Animals

Adult male CD1 mice (8–12 weeks old) were housed at 23±2°C under a 12 h light/dark cycle with ad libitum access to standard laboratory chow and water. For in vivo experiments, animals were deprived of food but were allowed access to water from 12 h before the start of the experiments.

Measurements of Ca^{2+} responses, mitochondrial membrane potential ($\Delta\Psi_M$) and IP_3 uncaging

Fresh pancreatic acinar cells were isolated as described.[7] Fluo 4-AM (3 μM), ci-IP_3/PM (2 μM) and/or tetramethyl rhodamine methyl ester (TMRM, 37.5 nM) were loaded for 30 min at room temperature. Confocal images were acquired on a Zeiss LSM510 system (Carl Zeiss Jena GmbH, Germany) with a 63× C-Apochromat water immersion objective (NA 1.2). $\Delta\Psi_M$ was recorded in the perigranular mitochondrial cell region. IP_3 was uncaged by UV excitation of whole cells (364 nm, 1% power) every three seconds where indicated. All fluorescence measurements were expressed as changes from basal fluorescence (F/F_0 ratio), where F_0 represents initial fluorescence at the start of each experiment.

In vitro necrosis assays

For CCK-induced cell death, a time-course propidium iodide (50 μM) necrosis assay was run at 37°C using a POLARstar Omega Plate Reader (BMG Labtech, Germany). Isolated murine pancreatic acinar cells (75 μL) were added to a caffeine solution (75 μL) at selected concentrations or the same volume of physiological saline (for controls) prior to CCK (50 nM) addition.

In TLCS-induced cell injury, an end-point propidium iodide (100 μg/mL) necrosis assay was employed. Cells were incubated with respective test solutions and agitated by rotary inversion for 30 min at 37°C, centrifuged (at 260 *g* for 2 min), resuspended and transferred to a microplate. Data were calculated as background-subtracted (cell-free blanks) percentage of total death (in 0.02% TritonX). Data were normalised to minimum and maximum fluorescence using the formula $(F\text{-}F_{max})/(F_{max} - F_{min})+1$. All experiments were in triplicate.

Determination of serum dimethylxanthine and trimethylxanthine levels by liquid chromatography-mass spectrometry

Serum was analysed on a QTRAP5500 hybrid triple-quadrupole/linear ion trap instrument with TurboIon V Ion source (Applied Biosystems, UK), with inline LC (Ultimate 3000 (Thermoscientific/Dionex, UK)) and Gemini C18, 3 μm, 2.1×100 mm column (Phenomenex, UK). Eluent A comprised

H_2O/0.1%, formic acid (FA)/1% and *tetrahydrofuran* v/v, Eluent B 100% acetonitrile/0.1% FA v/v. The QTRAP5500 was operated in positive electrospray ionisation (ESI) mode and two MRM transitions were monitored for caffeine (195.3/138.0 and 195.3/110.0), theobromine (181.1/124.0 and 181.1/96.0), paraxanthine (181.2/124.0 and 181.2/142.0), theophylline (181.7/96.0 and 181.7/124.0) and internal standard (paracetamol—152.064/110.0 and 152.064/65.0) with a 100 ms dwell time. Also, 1 μL of 100 μM internal standard was added to 50 μL of each mouse serum sample and subjected to acetone precipitation (8:1 v/v) at −20°C for 1 h. Samples were centrifuged at 14 000*g* for 10 min at 4°C, then supernatant vacuum centrifuged to a volume of 50 μL. A 10 μL aliquot was injected into the liquid chromatography-mass spectrometry system. All xanthine serum concentrations were determined using a calibration curve of 1–100 μM for each analyte, spiked in mouse serum.

Experimental AP

Hyperstimulation AP was induced by either 7 or 12 intraperitoneal injections of 50 μg/kg caerulein hourly (CER-AP), with saline controls. Bile acid AP was induced by retrograde infusion of 50 μL taurolithocholate acid sulfate (3 mM, TLCS-AP) into the pancreatic duct as described, with saline injection (sham) controls.[10 36] FAEE-AP was induced by simultaneous intraperitoneal injection of ethanol (1.35 g/kg) and palmitoleic acid (POA, 150 mg/kg), twice at 1 h apart.[7] Control mice received only ethanol (1.35 g/kg) injections. In all models, analgesia with 0.1 mg/kg buprenorphine hydrochloride (Temgesic, Reckitt and Coleman, Hull, England) was administered. Mice were humanely killed at designated time points for determination of severity (see online supplementary materials and methods).

Caffeine administration in vivo

Details of caffeine dose optimisation and administration of other methylxanthines are described in supplementary materials and methods. In CER-AP, mice received seven intraperitoneal injections of 1, 5, 10 or 25 mg/kg of caffeine (called regimen subsequently) hourly, beginning 2 h after the first caerulein injection, and were humanely killed at 12 h for determination of severity. The effect of caffeine was also assessed in both 7-injection and 12-injection CER-AP models at 24 h. In TLCS-AP, caffeine (25 mg/kg regimen) was begun 1 h after TLCS infusion and severity determined after humane killing at 24 h. In FAEE-AP, two intraperitoneal injections of caffeine (25 mg/kg, 1 h apart) were administered from an hour after the second POA/ethanol injection.

Statistical analysis

Results are presented as means±SEM from three or more independent experiments. In all figures, vertical bars denote mean ±SE values. Statistical analysis was performed using Student's t test or analysis of variance in Origin 8.5 (OriginLab, Northampton, Massachusetts, USA) and a value of $p<0.05$ considered significant.

Chemicals

Fluo 4-AM, TMRM and Hoechst 33342 were from Thermo Fisher Scientific (Waltham, Massachusetts, USA); ci-IP_3/PM from SiChem GmbH (Bremen, Germany). Unless otherwise stated, all other chemicals were from Sigma (Gillingham, UK) of the highest grade available.

RESULTS

Inhibition of ACh-induced $[Ca^{2+}]_C$ oscillations by caffeine and its dimethylxanthine metabolites

ACh (50 nM) caused $[Ca^{2+}]_C$ oscillations in pancreatic acinar cells that were concentration-dependently inhibited by caffeine at 500 μM to 2 mM (figure 1Ai, ii); 200 μM caffeine resulted in no significant reduction (data not shown). ACh-induced $[Ca^{2+}]_C$ oscillations were also inhibited by 500 μM theophylline (figure 1Aiii) and 500 μM paraxanthine (figure 1Aiv); all dimethylxanthines inhibited ACh-induced $[Ca^{2+}]_C$ signals in a concentration-dependent manner (figure 1Av). Theophylline, paraxanthine and theobromine induced significantly more inhibition than caffeine at 500 μM, with paraxanthine showing the highest potency. In contrast, 1-methylxanthine and xanthine showed minimal inhibition (see online supplementary figure S1A, B).

Inhibition of IP_3-mediated $[Ca^{2+}]_C$ signals by caffeine and its dimethylxanthine metabolites

To investigate whether methylxanthines might directly inhibit IP_3R-mediated Ca^{2+} elevations, a membrane-permeable caged IP_3 analogue, ci-IP_3/PM, was loaded into pancreatic acinar cells. Repetitive uncaging of ci-IP_3/PM caused sustained increases of $[Ca^{2+}]_C$ that were inhibited in a concentration-dependent manner by caffeine (3 and 5 mM) (figure 1Bi, ii). Theophylline and paraxanthine showed similar effects (figure 1Biii). These results suggest that methylxanthines inhibit IP_3R-mediated $[Ca^{2+}]_C$ signals by an action on the IP_3R.

Caffeine-induced inhibition of CCK-induced $[Ca^{2+}]_C$ signals, $\Delta\Psi_M$ loss and cell death

The effects of caffeine on CCK-induced toxic, sustained $[Ca^{2+}]_C$ signals were investigated. An elevated Ca^{2+} plateau followed hyperstimulation with 10 nM CCK (figure 2A), which was reduced by 27% by 1 mM caffeine (figure 2Ai), and blocked by 10 mM (figure 2Aii), effects reversible upon washout. Similar effects were observed when 10 mM caffeine was applied prior to 10 nM CCK stimulation (see online supplementary figure S2A).

Methylxanthines are PDE inhibitors and simultaneous increases in cAMP and cGMP may synergistically inhibit $[Ca^{2+}]_C$ oscillations induced by ACh.[37] The potential contribution of PDE inhibition to the effects of caffeine on CCK-induced sustained Ca^{2+} signals was investigated using non-hydrolysable analogues of cAMP and cGMP. Addition of 8-bromo-cAMP/GMP (1 mM) did not affect the CCK-induced $[Ca^{2+}]_C$ plateau, whereas 10 mM caffeine caused complete inhibition (figure 2B), suggesting a mechanism independent of intracellular cyclic nucleotide levels, although both xanthine and non-xanthine PDE inhibitors were found to inhibit ACh-induced $[Ca^{2+}]_C$ oscillations (see online supplementary figure S3A–D).

To test potential effects of caffeine on SOCE, internal Ca^{2+} stores were depleted under Ca^{2+}-free conditions using either 10 nM CCK or 2 μM thapsigargin, an inhibitor of the sarco-endoplasmic reticulum calcium transport ATPase (SERCA) and SOCE triggered by reapplication of extracellular Ca^{2+} (5 mM). Following depletion of internal stores with thapsigargin, caffeine was unable to revert the SOCE-induced Ca^{2+} plateau (figure 2Ci). When 10 nM CCK was used to deplete internal stores, the sustained SOCE plateau was significantly inhibited by 10 mM caffeine in a reversible manner (figure 2Cii). Following application of both CCK and thapsigargin, caffeine did not reduce the associated SOCE (figure 2Ciii). These data, summarised in figure 2Civ, are consistent with an

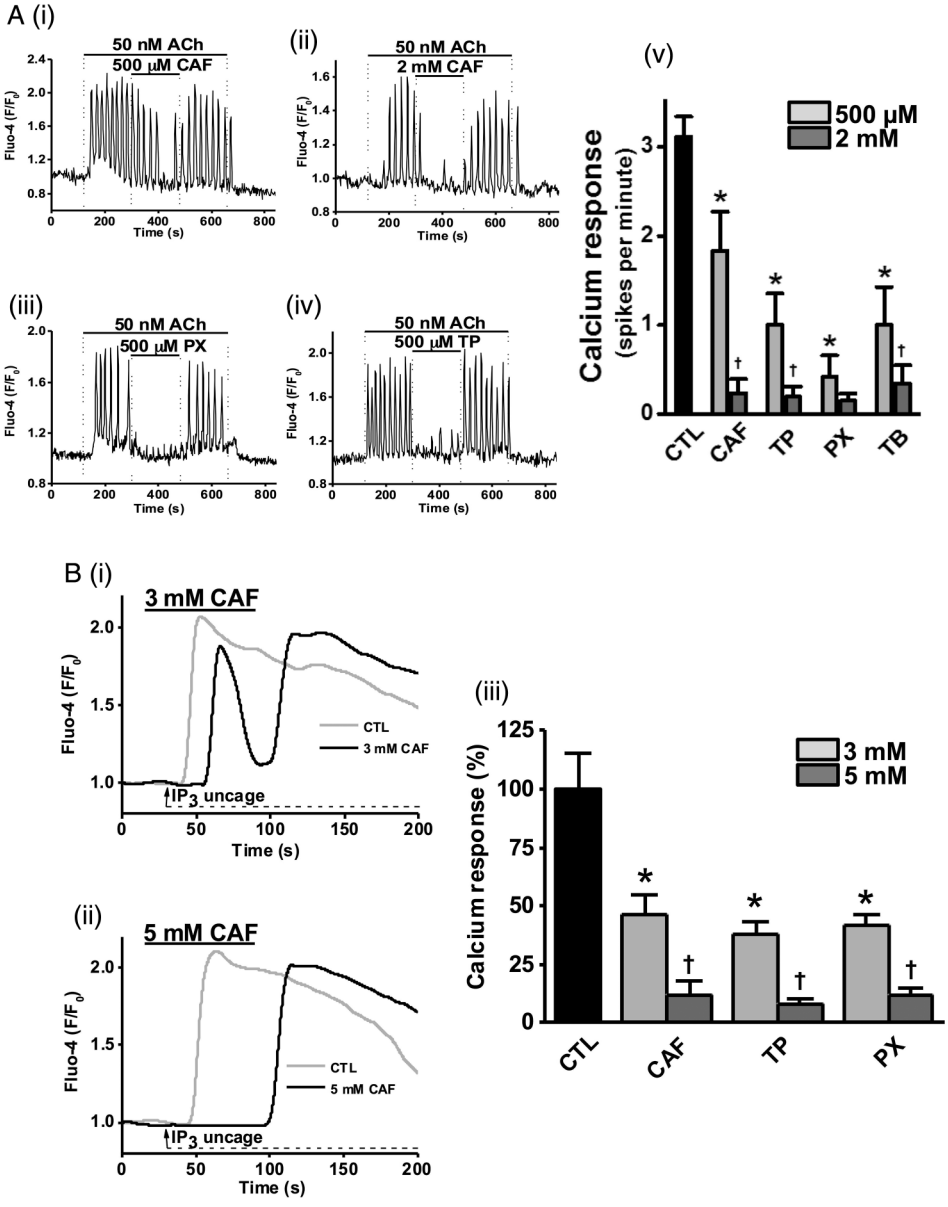

Figure 1 Dimethylxanthine and trimethylxanthines inhibit acetylcholine (ACh)-induced and inositol 1,4,5-trisphosphate receptor (IP_3)-induced Ca^{2+} signals in isolated pancreatic acinar cells. (A) Representative traces of ACh (50 nM) induced Ca^{2+} oscillations that were significantly inhibited by caffeine (CAF), theophylline (TP) and paraxanthine (PX): (i) partial inhibition by CAF at 500 μM, (ii) almost complete inhibition by CAF at 2 mM, or (iii) TP at 500 μM or (iv) PX at 500 μM. (v) Summary histograms of the inhibitory effects of CAF, TP, PX and theobromine (TB) on ACh-induced Ca^{2+} oscillations at both 500 μM and 2 mM. (B) Representative traces of Ca^{2+} elevations (grey) generated by uncaging of the membrane permeable IP_3 analogue, ci-IP_3/PM (2 μM) that were significantly inhibited by CAF (black): (i) partial inhibition at 3 mM and (ii) complete inhibition at 5 mM. (iii) Summary histograms of inhibitory effects of CAF, TP and PX on IP_3-induced Ca^{2+} elevations at 3 and 5 mM. *p<0.05 vs control group; †p<0.05 vs lower concentration. Traces are averages of >20 cells from at least three repeat experiments. Data normalised from basal fluorescence levels (F/F_0) and are expressed as means±SE in histograms.

inhibitory action of caffeine on IP_3R-mediated signalling, not SOCE per se.

Since sustained $[Ca^{2+}]_C$ elevations are known to induce mitochondrial dysfunction leading to pancreatic acinar cell necrosis,[6 7 10] the effects of caffeine on $\Delta\Psi_M$ were also evaluated. Caffeine (both 1 and 10 mM) did not significantly affect $\Delta\Psi_M$ on its own (figure 2Di), but it (10 mM) inhibited the loss of $\Delta\Psi_M$ induced by CCK, reversible on removal of the xanthine (figure 2Dii). In a time-course necrotic cell death pathway activation assay, caffeine (2 and 5 mM) reduced 50 nM CCK-induced cell death in a concentration-dependent and time-dependent manner (figure 2E).

Inhibition of TLCS-induced $[Ca^{2+}]_C$ signals and cell death by caffeine and its dimethylxanthine metabolites

To investigate effects of caffeine on bile acid induced $[Ca^{2+}]_C$ signals, 500 μM TLCS was applied to induce sustained $[Ca^{2+}]_C$ elevations in pancreatic acinar cells. Caffeine concentration-dependently blocked these TLCS-induced $[Ca^{2+}]_C$ elevations. Thus, 3 mM caffeine partially reduced the plateau (figure 3Ai), 5 mM caffeine further reduced the sustained elevation with oscillatory $[Ca^{2+}]_C$ rises sometimes superimposed (figure 3Aii), while 10 mM completely blocked the sustained elevations (figure 3Aiii). Pretreatment of cells with 10 mM caffeine converted 500 μM TLCS-induced $[Ca^{2+}]_C$ plateaus into oscillations (see online supplementary figure S2B).

The effects of methylxanthines on TLCS-induced necrosis were investigated using an end-point assay. Caffeine, theophylline and paraxanthine concentration-dependently inhibited TLCS-induced toxicity (figure 3Bi–iii). Caffeine induced a slight but significant reduction of TLCS-induced necrosis at 5 mM and approximately halved this at 10 mM (figure 3Bi). Similar patterns were observed for theophylline and paraxanthine over the range of concentrations tested (figure 3Bii, iii).

Serum dimethylxanthine and trimethylxanthine levels in CER-AP

The major metabolites of caffeine that appear in the blood stream of both humans and rodents are theophylline, paraxanthine, theobromine and monomethylxanthines (figure 4A). The serum levels of these were measured following in vivo caffeine administration to mice (25 mg/kg regimen) during

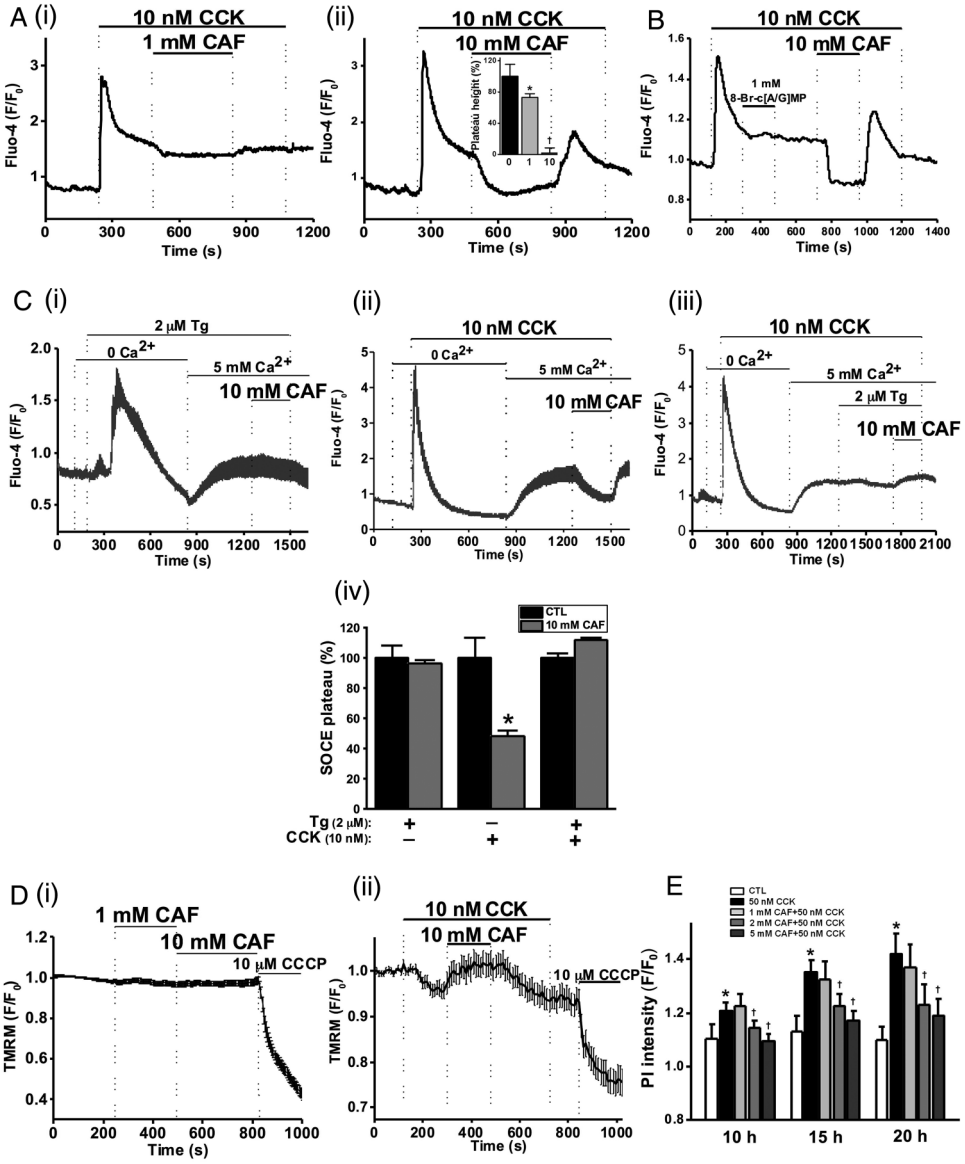

Figure 2 Caffeine (CAF) inhibits cholecystokinin (CCK)-induced sustained Ca^{2+} signals, mitochondrial membrane potential ($\Delta\Psi_M$) loss and cell death. (A) Representative traces showing the CCK-induced (10 nM) Ca^{2+} plateau that was significantly inhibited by CAF: (i) partial inhibition at 1 mM and (ii) almost complete inhibition at 10 mM, with mean plateau height as % above baseline (inset) showing CAF has a dose-dependent inhibitory effect on the plateau height (*p<0.05 vs control group; †p<0.05 vs lower concentration). (B) Representative trace showing the lack of inhibitory effect of non-hydrolysable analogues of cyclic adenosine monophosphate (cAMP) and cyclic guanosine monophosphate (cGMP), 8-bromo-cAMP/cGMP (1 mM) on the CCK-induced Ca^{2+} plateau, subsequently abolished by CAF (10 mM). (C) Representative traces and summary histogram showing that CAF (10 mM) (i) did not inhibit the store-operated Ca^{2+} entry plateau (SOCE) induced by thapsigargin (TG, 2 μM) but (ii) did inhibit SOCE induced by CCK (10 nM); (iii) CAF did not inhibit SOCE in the presence of TG. (iv) Summary histogram of the effect of CAF on the SOCE plateau in the presence of TG, CCK, or both (*p<0.05 vs control group). (D) Loss of mitochondrial $\Delta\Psi_M$ (tetramethyl rhodamine methyl, TMRM) induced by CCK (10 nM) was reversed by application of CAF (10 mM), after removal of which the $\Delta\Psi_M$ dropped once more and addition of the protonophore (CCCP, 10 μM) collapsed this to a minimal level: (i) CAF itself had no significant effect on $\Delta\Psi_M$; (ii) effect on CAF on CCK-induced $\Delta\Psi_M$ loss. (E) CAF significantly inhibited necrotic cell death pathway activation (PI uptake) induced by CCK (50 nM) in a dose-dependent manner at 2 and 5 mM (*p<0.05 vs control group; †p<0.05 vs CCK only). Traces are averages of >19 cells from at least three repeat experiments. Data normalised from basal fluorescence levels (F/F_0) and are expressed as means±SE in histograms.

CER-AP. The serum levels of caffeine were up to 700 μM at 10 min after four caffeine injections (figure 4B). It peaked at 10 min after seven injections of caffeine at >1 mM and gradually reduced to >600 and >400 μM at 2 and 6 h after last caffeine injection, respectively (figure 4B). Caffeine was the most abundant xanthine detected (~1200 μM 10 min after seven injections), followed by theobromine (~400 μM), theophylline (~300 μM) and paraxanthine (~150 μM) (figure 4C). The total level of dimethylxanthine and trimethylxanthine rose to >2 mM, a concentration capable of exerting marked inhibition of CCK-induced Ca^{2+} signals and cell death.

Effects of dimethylxanthine and trimethylxanthine on the severity of CER-AP

Since caffeine and its dimethylxanthine metabolites were able to protect against Ca^{2+}-induced toxicity in vitro, an evaluation of caffeine was carried out in vivo on CER-AP. In the CER-AP with seven caerulein injections, at 12 h after the first caerulein

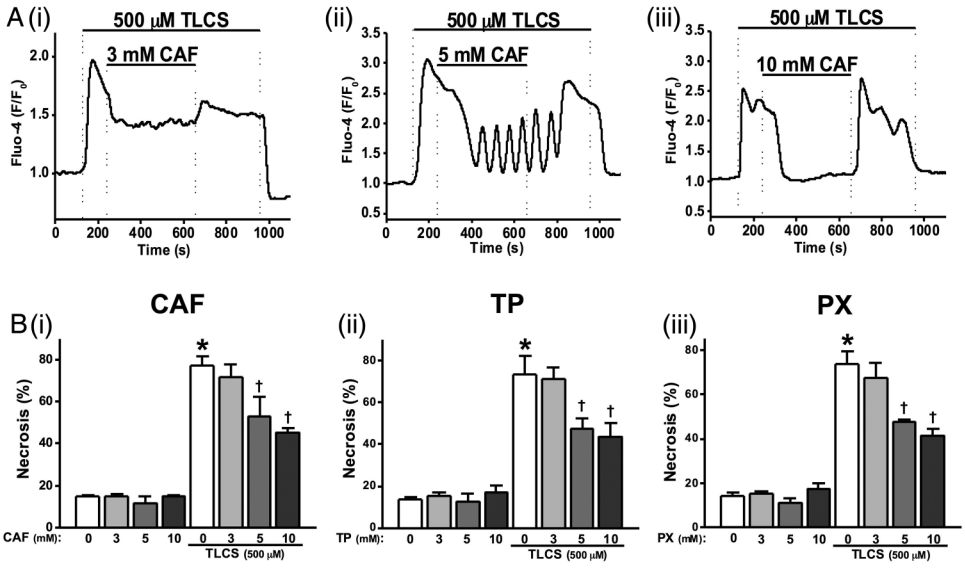

Figure 3 Effects of methylxanthines on taurolithocholic acid 3-sulfate (TLCS)-induced Ca^{2+} signals and cell death. (A) Representative traces showing that the TLCS-induced (500 μM) Ca^{2+} plateau was significantly inhibited by caffeine (CAF): (i) partial inhibition at 3 mM, (ii) the sustained Ca^{2+} plateau was converted to oscillations at 5 mM and (iii) complete inhibition at 10 mM. (B) (i) CAF significantly inhibited necrotic cell death pathway activation (PI uptake) induced by TLCS (500 μM) in a dose-dependent manner at 5 and 10 mM. Similar effects were also seen for (ii) theophylline (TP) and (iii) paraxanthine (PX). CAF, TP and PX did not affect basal PI uptake compared with normal controls (*p<0.05 vs control group; †p<0.05 vs TLCS only). Traces are averages of >20 cells from at least three repeat experiments. Data normalised from basal fluorescence levels (F/F_0) for Ca^{2+} signals and from maximal fluorescence levels (F/F_{max}) for PI uptake, respectively. Data are expressed as means±SE in histograms.

injection there were significant elevations of serum amylase, pancreatic oedema (pancreatic wet to dry ratio), trypsin and myeloperoxidase (MPO) activity (a marker of neutrophil infiltration), with increases of lung MPO activity, alveolar membrane thickening and serum interleukin (IL)-6 (figure 5A–F and online supplementary figure S4A, B). To evaluate possible further distant organ injury, we assessed renal pathology in CER-AP, but no significant effects were seen on serum creatinine and renal histology, which appeared normal (see online supplementary figure S4C, D). Typical histopathological features of AP (oedema, vacuolisation, neutrophil infiltration and necrosis) were confirmed and mirrored by histopathology scores (figure 5G, H).

In agreement with in vitro findings, there was dose-dependency for caffeine in ameliorating the severity of CER-AP (figure 5A–F). Using 1 mg/kg caffeine regimen, there was no significant effect; with 5 mg/kg caffeine, there was significant reduction of pancreatic oedema and MPO activity, although other parameters remained unchanged. With 10 and 25 mg/kg caffeine regimens, there was marked suppression of serum amylase, pancreatic oedema, trypsin and MPO activity, whereas elevated lung MPO activity, alveolar membrane thickening and elevated serum IL-6 levels remained unsuppressed (figure 5A–F and online supplementary figure 4B). Caffeine had no significant effect on serum creatinine and renal histology (see online supplementary figure S4C, D). Caffeine at both 10 and 25 mg/kg markedly reduced the overall histopathology score (figure 5Hi). The protective effect at 25 mg/kg was the most marked (figure 5G), confirmed by the histopathological scores (figure 5Hii–iv). In other experimental AP models, the 25 mg/kg regimen was used, reduced to two injections for FAEE-AP.

To determine whether caffeine reduced pancreatic injury through direct vascular actions that increased blood flow,[38] we determined pancreatic blood flow using fluorescent microspheres in untreated animals (see online supplementary materials and methods), in CER-AP and in CER-AP following 25 mg/kg caffeine regimen. While CER-AP markedly reduced pancreatic blood flow, caffeine did not have a significant effect on this flow, although there was a trend towards a modest improvement (see online supplementary figure S4E).

In contrast of the dramatic effects of caffeine on caerulein-induced pancreatic injury, theophylline and paraxanthine did not exert significant protective effects in CER-AP with both 10 and 25 mg/kg regimens (see online supplementary figure S5A–E). To further explore these unexpected findings, the serum levels of theophylline and paraxanthine were measured from both dose regimens. Serum levels of theophylline and paraxanthine 10 min after the last xanthine injection were each <100 μM in the 25 mg/kg regimen and <50 μM in the 10 mg/kg regimen (see online supplementary figure S6). These dimethylxanthine concentrations were previously shown not to alter IP_3R-mediated $[Ca^{2+}]_C$ signals in vitro, consistent with an effect of caffeine on this signalling pathway.

Since caffeine treatment was markedly protective in CER-AP at 12 h after induction by seven caerulein injections, its effects on more severe disease at a later time point were compared (figure 6). CER-AP induced by 12 hourly caerulein injections converted mild necrotising AP into a severe necrotising form characterised by extensive pancreatic oedema, neutrophil infiltration and necrosis at 24 h after induction (figure 6Ei–iv). Caffeine (25 mg/kg regimen) markedly reduced all parameters of pancreatic injury in both models.

Protective effects of caffeine on TLCS-AP and FAEE-AP

TLCS-AP caused dramatic increases of pancreatic and systemic injury markers compared with the sham group at 24 h (figure 7A–E), with marked histopathological changes (figure 7F). Since pancreatic trypsin activity peaks very early after induction of AP in the bile acid-induced model, this parameter was not included for severity assessment.[36] Caffeine significantly reduced serum amylase (figure 7A), pancreatic oedema (figure 7B),

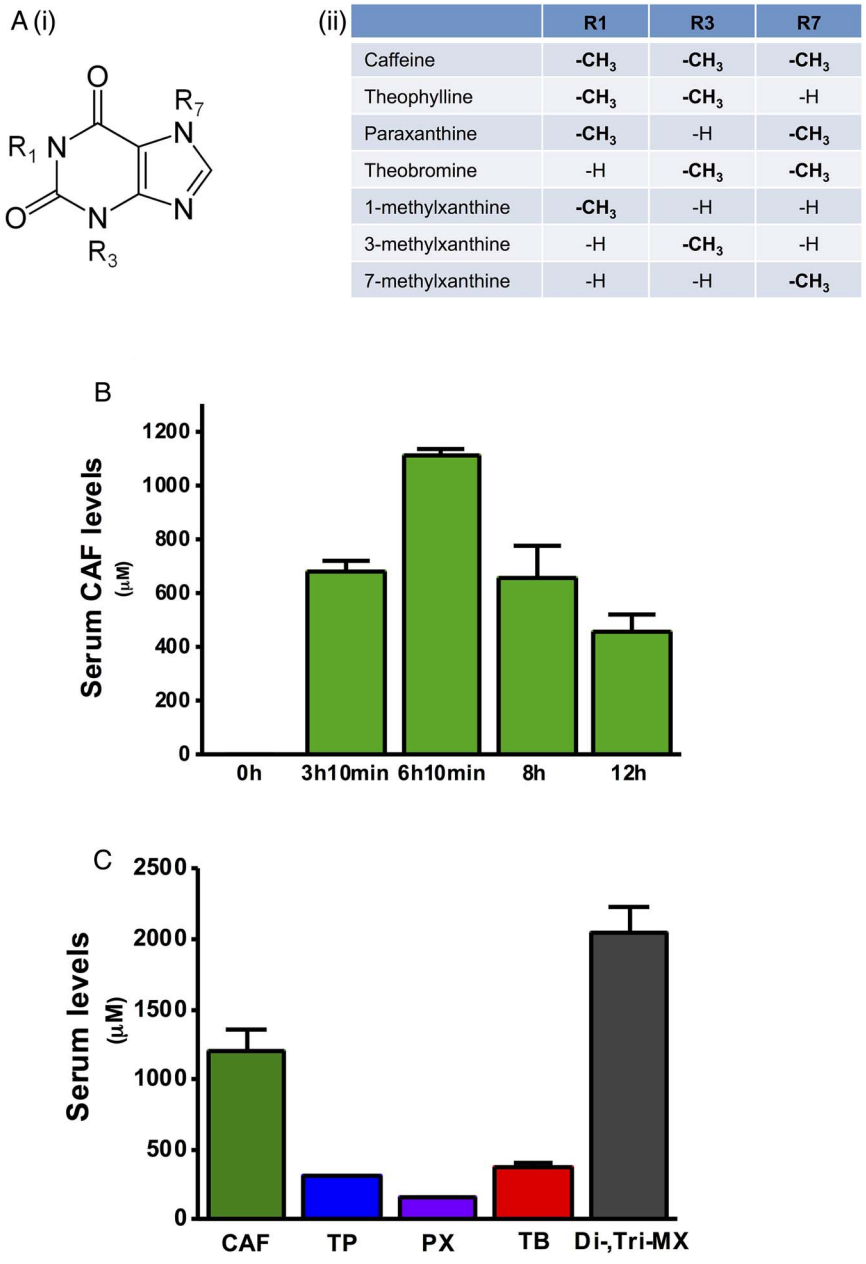

	R1	R3	R7
Caffeine	$-CH_3$	$-CH_3$	$-CH_3$
Theophylline	$-CH_3$	$-CH_3$	-H
Paraxanthine	$-CH_3$	-H	$-CH_3$
Theobromine	-H	$-CH_3$	$-CH_3$
1-methylxanthine	$-CH_3$	-H	-H
3-methylxanthine	-H	$-CH_3$	-H
7-methylxanthine	-H	-H	$-CH_3$

Figure 4 Methylxanthine (MX) structure and determination of serum di-MX and tri-MX levels in caerulein acute pancreatitis (CER-AP). (A) (i) Positions 1, 3 and 7 methylation of the xanthine structure are shown. (ii) Dependent on methylation state, caffeine (CAF) and its MX metabolites are classed as mono-MX, di-MX and tri-MX that are listed in the table. (B) In CER-AP, caffeine at 25 mg/kg (seven injections hourly) was given simultaneously with each CER (50 μg/kg) injection. Mice were sacrificed at different time points to measure serum caffeine (CAF, tri-MX) levels by LC/MS. (C) Respective serum di-MX levels and total di-MX and tri-MX levels showing peak caffeine concentration at 10 min after last caffeine/CER injection: CAF had the highest serum concentration, followed by theobromine (TB), theophylline (TP) and paraxanthine (PX). The cumulative concentration of di-MX and tri-MX was >2 mM. Values are means±SE from six mice.

pancreatic MPO activity (figure 7C) and serum IL-6 (figure 7E), but did not affect lung MPO activity (figure 7D). Caffeine significantly reduced the overall histopathological score (figure 7Gi), as well as the specific oedema (figure 7Gii) and inflammation scores (figure 7Giii), with a trend to curtail the necrosis score (figure 7Giv).

Since caffeine inhibits FAEE-induced Ca^{2+} signals in vitro,[7] its effects in FAEE-AP were tested. Co-administration of ethanol and POA caused typical AP features compared with ethanol alone (figure 8A–G).[7] Two injections of 25 mg/kg caffeine significantly reduced serum amylase, pancreatic oedema, trypsin and MPO activity, although an increase in lung MPO activity was observed (figure 8A–E). The overall histopathological score (figure 8Gi) was greatly ameliorated, with significantly lowered oedema (figure 8Gii) and inflammation (figure 8Giii) with a trend towards a decrease in necrosis (figure 8Giv).

DISCUSSION

This study defines the inhibitory effects of methylxanthines on IP_3R-mediated Ca^{2+} release from the pancreatic acinar endoplasmic reticulum store into the cytosol and their potential application in AP. It has been shown that caffeine inhibits IP_3Rs[29] as well as IP_3 production in a concentration-dependent manner.[28] We found that inhibition of IP_3R-mediated Ca^{2+} release is attributable at least in part to an action on the IP_3R, since xanthines inhibited IP_3R-mediated Ca^{2+} release elicited by uncaged IP_3. Caffeine, theophylline and paraxanthine prevented physiological Ca^{2+} signalling and toxic elevations of $[Ca^{2+}]_C$ induced by agents (CCK and TLCS) that cause AP, in a concentration-dependent manner (500 μM to 10 mM), also inhibiting falls in $\Delta\Psi_M$ and necrotic cell death pathway activation. An inhibitory action on PDE preventing cAMP/cGMP degradation could not account for the effects on toxic $[Ca^{2+}]_C$ overload since additional cAMP/cGMP did not prevent these. Extending these findings in vivo, caffeine significantly reduced the severity of multiple, diverse models of AP. The combined concentrations of dimethylxanthine and trimethylxanthine after the 25 mg/kg caffeine protocol were within the range over which effects on both IP_3R-mediated Ca^{2+} release and toxic elevations of $[Ca^{2+}]_C$ were identified. Despite the half-life of

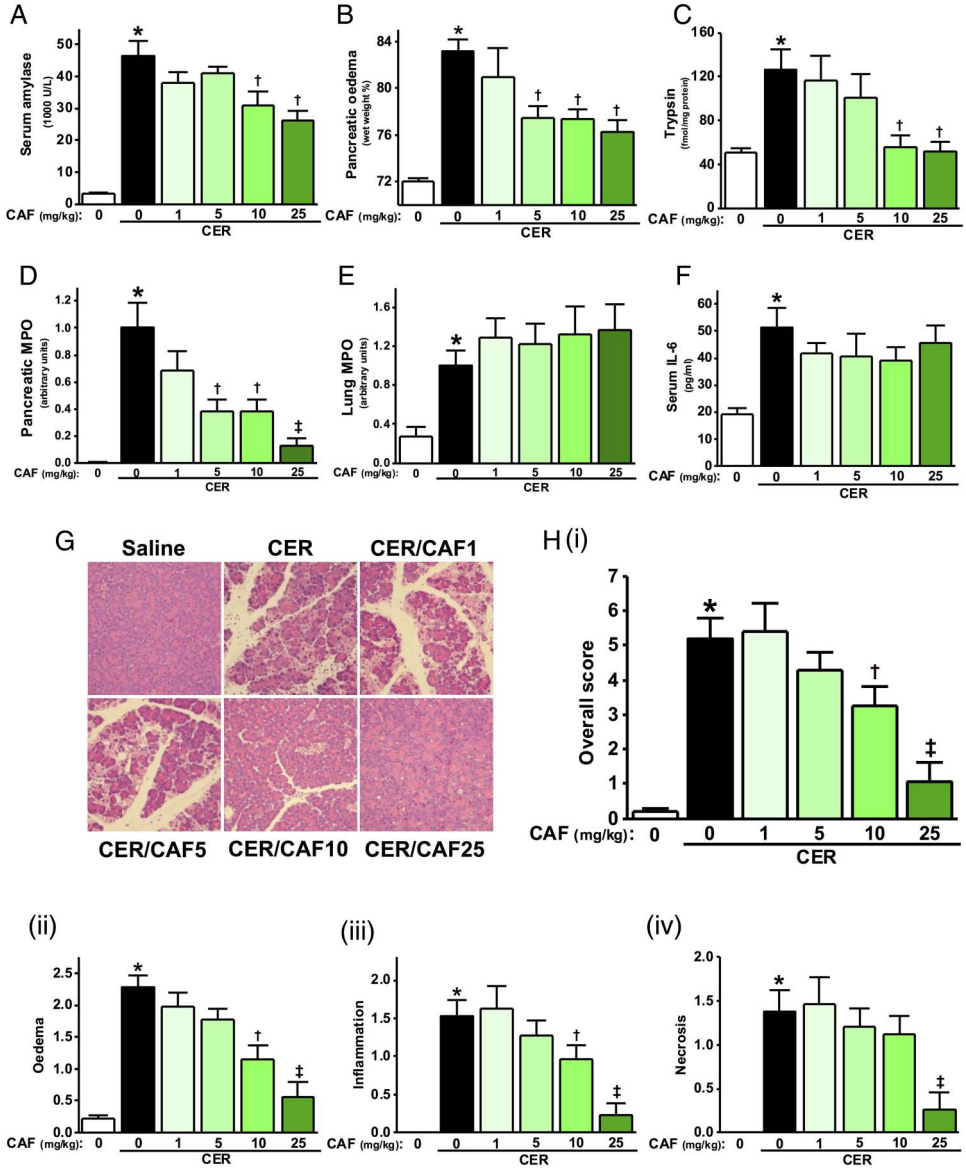

Figure 5 Dose-dependent protective effects of caffeine on the severity of caerulein acute pancreatitis (CER-AP) at 12 h. Mice received either intraperitoneal injections of 50 μg/kg CER (seven injections hourly) or equal amount of saline injections. Caffeine (CAF) at 1, 5, 10 or 25 mg/kg regimen (seven injections hourly) was begun 2 h after the first injection of CER. Mice were sacrificed at 12 h after disease induction and assessed for (A) serum amylase, (B) pancreatic oedema, (C) pancreatic trypsin activity, (D) pancreatic myeloperoxidase (MPO) activity (normalised to CER group), (E) lung MPO activity (normalised to CER group) and (F) serum interleukin (IL-6). (G) Representative images of pancreatic histopathology for all groups (H&E, ×200). (H) (i) Overall histopathological score and components: (ii) oedema, (iii) inflammation and (iv) necrosis. *p<0.05 vs control group; †p<0.05 vs CER group. Values are means±SE of 6–8 animals per group.

caffeine in mice of ~60 min,[39] the combined peak concentrations of dimethylxanthine and trimethylxanthine with the 25 mg/kg caffeine regimen were >2 mM, and serum caffeine was >400 μM 6 h after last caffeine injection. Following similar protocols of 25 mg/kg theophylline or paraxanthine, concentrations were far below the effective range on IP_3Rs but within the effective range on PDE (approaching 100 μM 10 min after the last dimethylxanthine injection),[26] and no protective effects on in vivo AP were seen. Nor were significant protective effects seen on pancreatic blood flow with the 25 mg/kg caffeine regimen, to be expected if mediated via PDE inhibition.[38] Since pancreatic cellular injury initiates and determines severity in AP, the protective effect of caffeine on AP is likely to have been mediated by inhibition of IP_3R-mediated Ca^{2+} release.

The concentration range over which caffeine inhibited toxic $[Ca^{2+}]_C$ overload induced by CCK hyperstimulation was similar to that seen here with quasi-physiological ACh-elicited Ca^{2+} oscillations, as previously in pancreatic acinar cells[28] and permeabilised vascular smooth muscle cells.[40] There could have been a cAMP/cGMP-dependent component to inhibition of the ACh-elicited Ca^{2+} oscillations since both xanthine-based and non-xanthine-based PDE inhibitors reduced ACh-elicited Ca^{2+} oscillations. Nevertheless, PDE inhibition is unlikely to have contributed to the reduction of toxic $[Ca^{2+}]_C$ overload as this was not affected by application of cell-permeable cAMP/cGMP analogues, but was immediately reversed upon caffeine administration. It is also unlikely that any increase in SERCA activity occurred in response to caffeine and downstream rises in cyclic nucleotide levels since no decrease in $[Ca^{2+}]_C$ was induced by

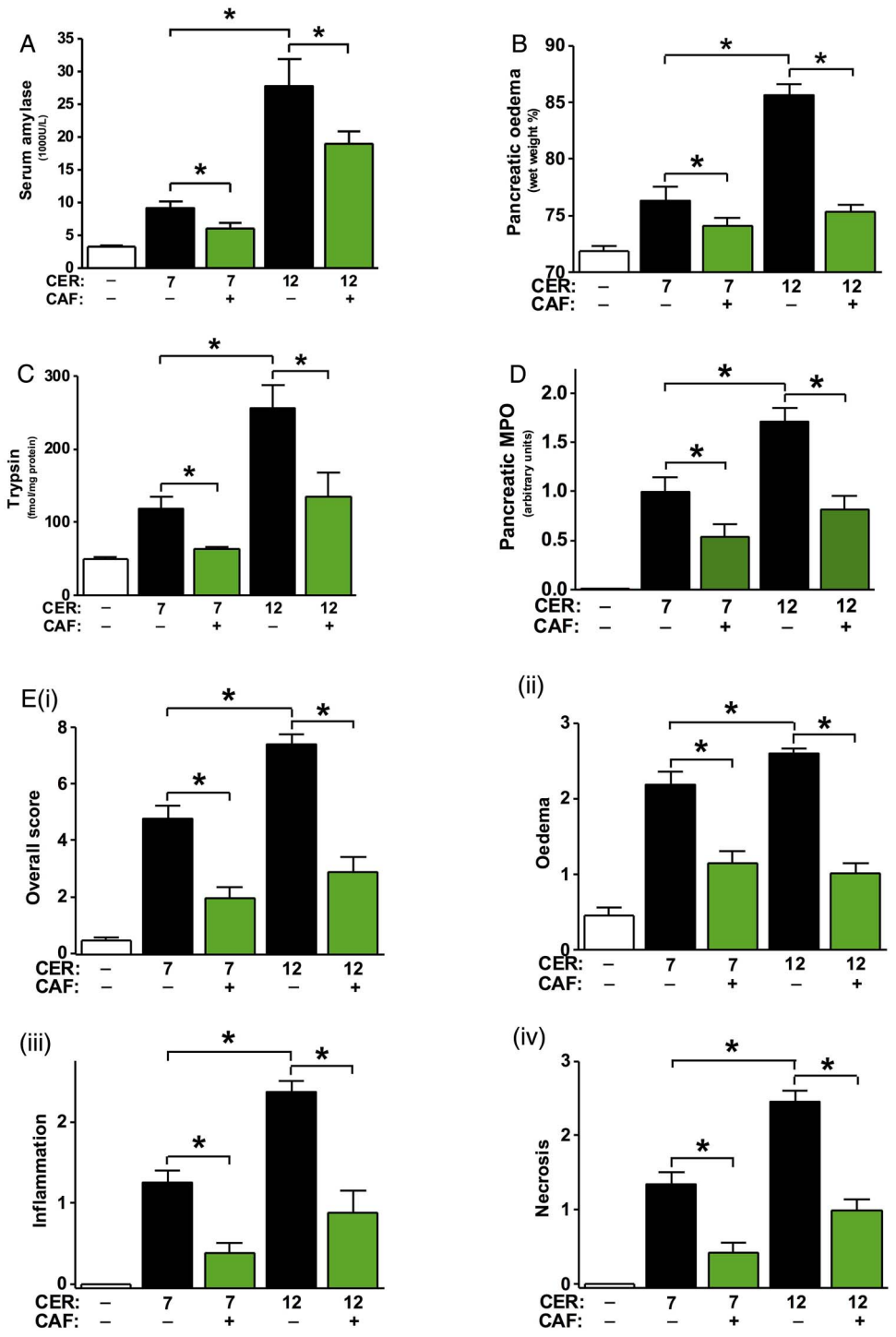

Figure 6 Caffeine (CAF) protects against pancreatic injury in two caerulein acute pancreatitis (CER-AP) models at 24 h. Mice received either intraperitoneal injections of 50 μg/kg CER (both 7 and 12 injections hourly) or equal amounts of saline injections. Caffeine (CAF) at the 25 mg/kg regimen (7 injections hourly) was begun 2 h after the first injection of CER. Mice were sacrificed at 24 h after disease induction and were assessed for (A) serum amylase, (B) pancreatic oedema, (C) pancreatic trypsin activity and (D) pancreatic myeloperoxidase (MPO) activity (normalised to CER group). (E) (i) Overall histopathological score and components: (ii) oedema, (iii) inflammation and (iv) necrosis. *Indicates $p<0.05$. Values are means ±SE of 6–8 animals per group.

analogues of cAMP and cGMP, which have been shown to upregulate SERCA via phospholamban.[41] Therefore, the actions of caffeine on toxic $[Ca^{2+}]_C$ overload are consistent with a primary effect on IP_3R-mediated Ca^{2+} release.

SOCE in pancreatic acinar and ductal cells occurs predominantly via Orai channels and is regulated in part by TRP channels.[42] Previously we found inhibition of Orai to markedly reduce CER-AP, TLCS-AP and FAEE-AP.[15] Inhibition of TRPC3 was found to reduce a mild model of CER-AP,[16] while the non-selective cation channel TRPV1[43 44] as well as TRPA1[44] have been implicated in neurogenic inflammation contributing to AP. We obtained no data to indicate any direct effect of caffeine on Orai or TRP channels. On the contrary, SOCE is unlikely to have been inhibited directly by caffeine since caffeine had no

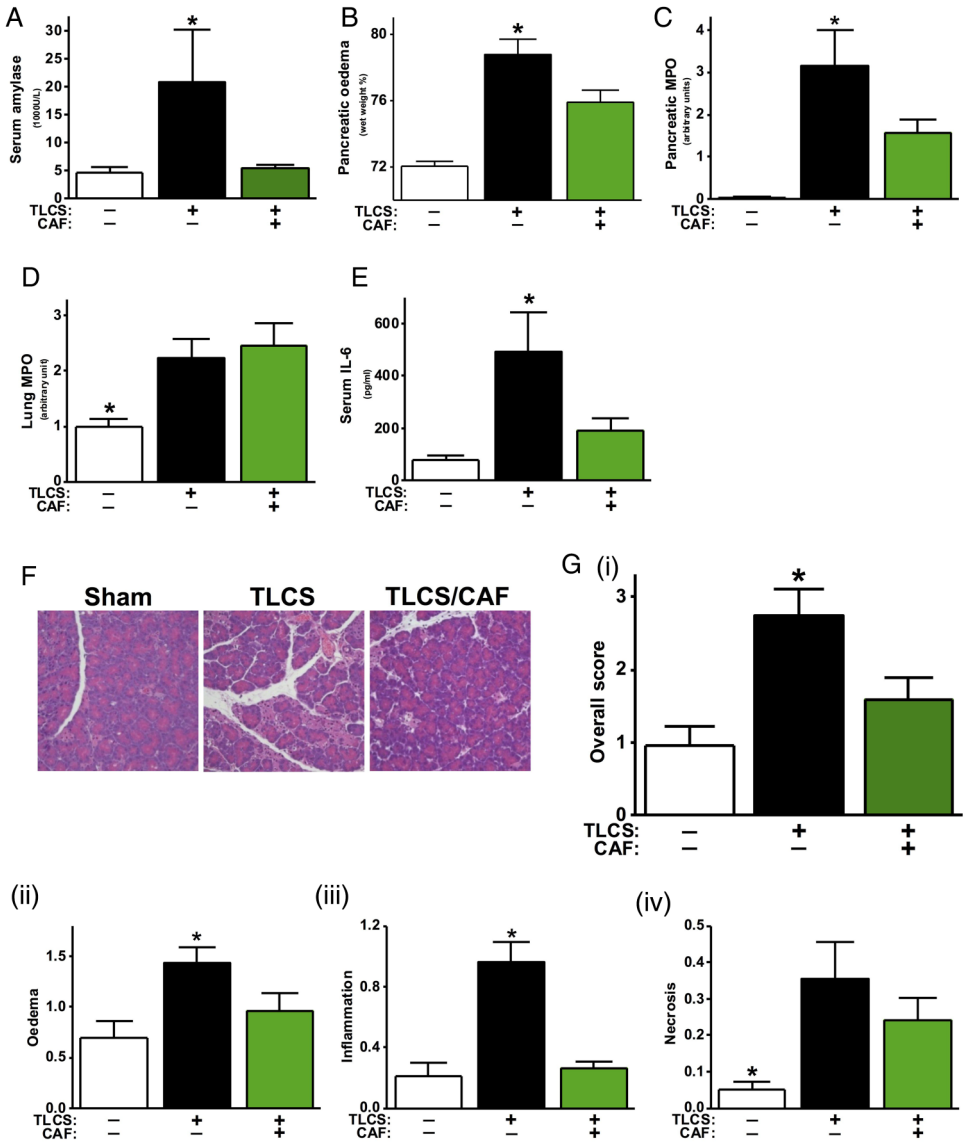

Figure 7 Protective effects of caffeine (CAF) on taurolithocholic acid 3-sulfate (TLCS)-acute pancreatitis (AP). Mice received either retrograde infusion of 50 μL of 3 mM TLCS into the pancreatic duct or underwent sham surgery. CAF at 25 mg/kg (seven injections hourly) was begun 1 h after TLCS infusion. Mice were sacrificed at 24 h after disease induction and were assessed for (A) serum amylase level, (B) pancreatic oedema, (C) pancreatic myeloperoxidase (MPO) activity (normalised to sham group), (D) lung MPO activity (normalised to sham group) and (E) serum interleukin (IL-6). (F) Representative pancreatic histopathology for all groups (H&E, ×200). (G) (i) Overall histopathological score and components: (ii) oedema, (iii) inflammation and (iv) necrosis. *p<0.05 vs other two groups. Values are means±SE of 6–11 animals per group.

effect on thapsigargin-induced $[Ca^{2+}]_C$ plateaus, rather SOCE will have been inhibited secondarily to reduction of store depletion, the principal driver of SOCE in non-excitable cells.[14 15 21]

Inhibition of second messenger-mediated Ca^{2+} release via RyR ameliorates both caerulein[45] and bile acid-induced AP.[46] Since caffeine enhances Ca^{2+} release from RyRs in excitatory cells,[32] and RyRs are major contributors to Ca^{2+} signalling in pancreatic acinar cells,[23 47] the effects of caffeine in the reduction of toxic Ca^{2+} overload observed here might appear contradictory. However, in contrast to the situation in muscle cells, caffeine can only release Ca^{2+} in pancreatic acinar cells under quite exceptional circumstances and then only when present at a low concentration (1 mM); indeed, this effect is abolished by stepping up the caffeine concentration.[29] Furthermore, ACh-elicited Ca^{2+} signalling is blocked by inhibiting IP_3Rs pharmacologically[29] and knockout of the principal subtypes (IP_3R2 and IP_3R3) results in a failure of Ca^{2+} signal generation and secretion.[20] Thus, caffeine is used extensively as an inhibitor of Ca^{2+} release in fundamental investigations of pancreatic acinar and other electrically non-excitable cells.[27]

Little, if any, protective effect of caffeine on experimental AP can be attributed to actions on adenosine receptors, which have both inhibitory (A1, A3) and excitatory (A2A, A2B) actions mediated in part through changes in cAMP.[48] Caffeine is an antagonist of all adenosine receptors; the potency of caffeine is highest on A2A then A1 receptors at concentrations 10–20 times lower than on PDE.[26] In the rat pancreas, few acinar cells express adenosine receptors;[49] differential subtype expression occurs in vascular endothelium, nerve fibres, islet cells and ductal cells, with total expression A2A>A2B>A3>A1.[48] While antagonism of the least predominant receptor (A1) previously reduced pancreatic oedema but no other parameter of experimental AP,[49] the majority of data indicate that increasing adenosine receptor activation by reuptake inhibition or administration

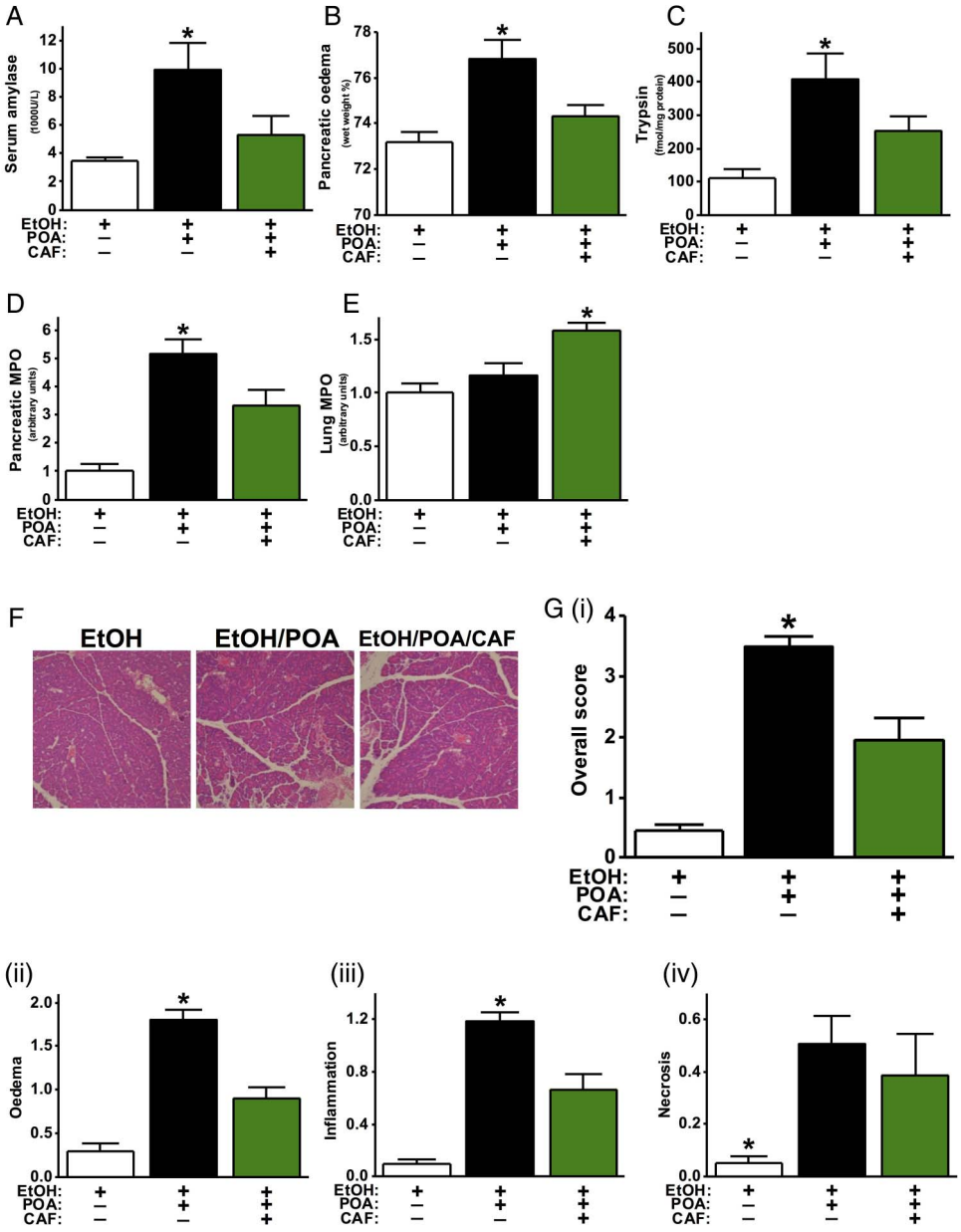

Figure 8 Protective effects of caffeine (CAF) on fatty acid ethyl ester acute pancreatitis. Mice received two intraperitoneal injections of ethanol (EtOH, 1.35 g/kg) in combination with palmitoleic acid (POA, 150 mg/kg) or equal amounts of EtOH injection only, 1 h apart. CAF at 25 mg/kg (seven injections hourly) was given 1 h after the second injection of EtOH/POA. Mice were sacrificed 24 h after disease induction and assessed for (A) serum amylase level, (B) pancreatic oedema, (C) pancreatic trypsin activity, (D) pancreatic myeloperoxidase (MPO) activity (normalised to EtOH group) and (E) lung MPO activity (normalised to EtOH group). (F) Representative pancreatic histopathology for all groups (H&E, ×200). (G) (i) Overall histopathological score and components: (ii) oedema, (iii) inflammation and (iv) necrosis. *p<0.05 vs other two groups. Values are means±SE of 10 animals per group.

of A2 or A3 receptor agonists ameliorates experimental AP.[50] Furthermore, adenosine receptor activation has broad anti-inflammatory effects, including reduction of neutrophil recruitment and effector functions via A2A and A2B;[51] antagonism of these receptors may account for the lack of effect of caffeine on lung MPO or lung histopathology in experimental AP. Similarly, protective effects via adenosine receptors would be expected at doses of caffeine that had no (1 mg/kg) or minimal (5 mg/kg) effect.[52]

High doses of caffeine were required to reduce the severity of experimental AP, with the most effective 25 mg/kg regimen extending into toxicity, indicative of a very narrow therapeutic index. At this dose, the number of hourly injections had to be reduced from seven to two in FAEE-AP to avoid mortality; in CER-AP, 50 mg/kg resulted in caffeine intoxication syndrome, although at 25 mg/kg no visible side effects were observed. In humans, even 10 mg/kg caffeine would be likely to induce caffeine intoxication, with florid neuro-excitotoxic and other undesirable side effects.[26] The principal caffeine metabolites in humans, monkeys, rabbits, rats and mice are similar and do not differ when given by mouth compared with intraperitoneally.[39] Paraxanthine, however, is the most abundant dimethylxanthine metabolite in humans, while in mice this is theobromine.[39] There is marked individual variability in caffeine metabolism

and pharmacokinetics;[26] since the half-life in humans typically ranges from 3 to 7 h, repeated high doses or continuous intravenous infusions would be hazardous unless rapid therapeutic monitoring were to be possible.

Our study has demonstrated proof of principle that caffeine causes marked amelioration of experimental AP, largely through inhibition of IP_3R-mediated signalling. Medicinal chemistry starting with the template of caffeine and/or other compounds that inhibit IP_3R-mediated signalling could lead to more potent, selective and safer drug candidates for AP.

Acknowledgements The authors thank Michael Neil and Robert Lee from the Department of Pathology, Royal Liverpool University Hospital, for processing histopathology samples; they also thank Mr Euan W McLaughlin for caffeine dose optimisation and Jane Armstrong for technical assistance.

Contributors WH and MCC are co-first authors. WH: acquisition of data; analysis and interpretation of data; drafting of the manuscript. MCC, RM, PS, XZ, VE, YO, MC, DL and LW: acquisition of data; analysis and interpretation of data. DMB: technical support; acquisition of data; analysis and interpretation of data; critical revision of the manuscript. ACH: material support; critical revision of the manuscript. OHP and AVT: critical revision of the manuscript; obtained funding. DNC: study concept and design; acquisition of data; analysis and interpretation of data; critical revision of the manuscript; study supervision. RS: study concept and design; analysis and interpretation of data; critical revision of the manuscript; obtained funding; study supervision.

Funding This work was supported by the Medical Research Council (UK), the Biomedical Research Unit funding scheme from the National Institute for Health Research and a State Administration of Traditional Chinese Medicine Key Discipline Construction Project.

Competing interests OHP is a MRC Professor; WH was a recipient of a UK/China Postgraduate Scholarship for Excellence and State Administration of Traditional Chinese Medicine Key Discipline Construction Project, China; MCC and DB were awarded MRC scholarships; RM was supported by an Amelie Waring Clinical Research Fellowship from CORE; PS was supported by The Royal Colleague of Surgeons of England Fellowship; XZ, YO and LW were supported by the China Scholarships Council.

Ethics approval Animal experiments were performed after ethical review and appropriate approval from the UK Home Office (PPL 40/3320) in accordance with the Animals (Scientific Procedures) Act 1986.

Provenance and peer review Not commissioned; externally peer reviewed.

Data sharing statement Upon publication raw data from individual experiments will be made available by the corresponding author to interested researchers requesting data for bona fide scientific purposes.

REFERENCES

1 Roberts SE, Akbari A, Thorne K, *et al*. The incidence of acute pancreatitis: impact of social deprivation, alcohol consumption, seasonal and demographic factors. *Aliment Pharmacol Ther* 2013;38:539–48.
2 Tenner S, Baillie J, DeWitt J, *et al*. American College of Gastroenterology guideline: management of acute pancreatitis. *Am J Gastroenterol* 2013;108:1400–15; 16.
3 Petersen OH, Tepikin AV. Polarized calcium signaling in exocrine gland cells. *Annu Rev Physiol* 2008;70:273–99.
4 Voronina SG, Gryshchenko OV, Gerasimenko OV, *et al*. Bile acids induce a cationic current, depolarizing pancreatic acinar cells and increasing the intracellular Na+ concentration. *J Biol Chem* 2005;280:1764–70.
5 Shalbueva N, Mareninova OA, Gerloff A, *et al*. Effects of oxidative alcohol metabolism on the mitochondrial permeability transition pore and necrosis in a mouse model of alcoholic pancreatitis. *Gastroenterology* 2013;144:437–46.e6.
6 Criddle DN, Murphy J, Fistetto G, *et al*. Fatty acid ethyl esters cause pancreatic calcium toxicity via inositol trisphosphate receptors and loss of ATP synthesis. *Gastroenterology* 2006;130:781–93.
7 Huang W, Booth DM, Cane MC, *et al*. Fatty acid ethyl ester synthase inhibition ameliorates ethanol-induced Ca2+-dependent mitochondrial dysfunction and acute pancreatitis. *Gut* 2014;63:1313–24.
8 Murphy JA, Criddle DN, Sherwood M, *et al*. Direct activation of cytosolic Ca2+ signaling and enzyme secretion by cholecystokinin in human pancreatic acinar cells. *Gastroenterology* 2008;135:632–41.
9 Criddle DN, Booth DM, Mukherjee R, *et al*. Cholecystokinin-58 and cholecystokinin-8 exhibit similar actions on calcium signaling, zymogen secretion, and cell fate in murine pancreatic acinar cells. *Am J Physiol Gastrointest Liver Physiol* 2009;297:G1085–92.
10 Mukherjee R, Mareninova OA, Odinokova IV, *et al*. Mechanism of mitochondrial permeability transition pore induction and damage in the pancreas: inhibition prevents acute pancreatitis by protecting production of ATP. *Gut* 2016;65:1333–46.
11 Saluja AK, Bhagat L, Lee HS, *et al*. Secretagogue-induced digestive enzyme activation and cell injury in rat pancreatic acini. *Am J Physiol* 1999;276(4 Pt 1):G835–42.
12 Raraty M, Ward J, Erdemli G, *et al*. Calcium-dependent enzyme activation and vacuole formation in the apical granular region of pancreatic acinar cells. *Proc Natl Acad Sci USA* 2000;97:13126–31.
13 Mooren F, Hlouschek V, Finkes T, *et al*. Early changes in pancreatic acinar cell calcium signaling after pancreatic duct obstruction. *J Biol Chem* 2003;278:9361–9.
14 Gerasimenko JV, Gryshchenko O, Ferdek PE, *et al*. Ca2+ release-activated Ca2+ channel blockade as a potential tool in antipancreatitis therapy. *Proc Natl Acad Sci USA* 2013;110:13186–91.
15 Wen L, Voronina S, Javed MA, *et al*. Inhibitors of ORAI1 prevent cytosolic calcium-associated injury of human pancreatic acinar cells and acute pancreatitis in 3 mouse models. *Gastroenterology* 2015;149:481–92.
16 Kim MS, Hong JH, Li Q, *et al*. Deletion of TRPC3 in mice reduces store-operated Ca2+ influx and the severity of acute pancreatitis. *Gastroenterology* 2009;137:1509–17.
17 Kim MS, Lee KP, Yang D, *et al*. Genetic and pharmacologic inhibition of the Ca2+ influx channel TRPC3 protects secretory epithelia from Ca2+-dependent toxicity. *Gastroenterology* 2011;140:2107–15.
18 Gerasimenko JV, Lur G, Sherwood MW, *et al*. Pancreatic protease activation by alcohol metabolite depends on Ca2+ release via acid store IP3 receptors. *Proc Natl Acad Sci USA* 2009;106:10758–63.
19 Lur G, Haynes LP, Prior IA, *et al*. Ribosome-free terminals of rough ER allow formation of STIM1 puncta and segregation of STIM1 from IP(3) receptors. *Curr Biol* 2009;19:1648–53.
20 Futatsugi A, Nakamura T, Yamada MK, *et al*. IP3 receptor types 2 and 3 mediate exocrine secretion underlying energy metabolism. *Science* 2005;309:2232–4.
21 Lur G, Sherwood MW, Ebisui E, *et al*. InsP(3)receptors and Orai channels in pancreatic acinar cells: co-localization and its consequences. *Biochem J* 2011;436:231–9.
22 Cancela JM, Van Coppenolle F, Galione A, *et al*. Transformation of local Ca2+ spikes to global Ca2+ transients: the combinatorial roles of multiple Ca2+ releasing messengers. *EMBO J* 2002;21:909–19.
23 Gerasimenko JV, Flowerdew SE, Voronina SG, *et al*. Bile acids induce Ca2+ release from both the endoplasmic reticulum and acidic intracellular calcium stores through activation of inositol trisphosphate receptors and ryanodine receptors. *J Biol Chem* 2006;281:40154–63.
24 Voronina S, Longbottom R, Sutton R, *et al*. Bile acids induce calcium signals in mouse pancreatic acinar cells: implications for bile-induced pancreatic pathology. *J Physiol* 2002;540:49–55.
25 Gerasimenko JV, Lur G, Ferdek P, *et al*. Calmodulin protects against alcohol-induced pancreatic trypsinogen activation elicited via Ca2+ release through IP3 receptors. *Proc Natl Acad Sci USA* 2011;108:5873–8.
26 Fredholm BB, Bättig K, Holmén J, *et al*. Actions of caffeine in the brain with special reference to factors that contribute to its widespread use. *Pharmacol Rev* 1999;51:83–133.
27 Petersen OH, Sutton R. Ca2+ signalling and pancreatitis: effects of alcohol, bile and coffee. *Trends Pharmacol Sci* 2006;27:113–20.
28 Toescu EC, O'Neill SC, Petersen OH, *et al*. Caffeine inhibits the agonist-evoked cytosolic Ca2+ signal in mouse pancreatic acinar cells by blocking inositol trisphosphate production. *J Biol Chem* 1992;267:23467–70.
29 Wakui M, Osipchuk YV, Petersen OH. Receptor-activated cytoplasmic Ca2+ spiking mediated by inositol trisphosphate is due to Ca2(+)-induced Ca2+ release. *Cell* 1990;63:1025–32.
30 Saleem H, Tovey SC, Molinski TF, *et al*. Interactions of antagonists with subtypes of inositol 1,4,5-trisphosphate (IP3) receptor. *Br J Pharmacol* 2014;171:3298–312.
31 Bezprozvanny I, Bezprozvannaya S, Ehrlich BE. Caffeine-induced inhibition of inositol(1,4,5)-trisphosphate-gated calcium channels from cerebellum. *Mol Biol Cell* 1994;5:97–103.
32 Ozawa T. Modulation of ryanodine receptor Ca2+ channels (Review). *Mol Med Rep* 2010;3:199–204.
33 Morton C, Klatsky AL, Udaltsova N. Smoking, coffee, and pancreatitis. *Am J Gastroenterol* 2004;99:731–8.
34 Wu MN, Ho K, Crocker A, *et al*. The effects of caffeine on sleep in Drosophila require PKA activity, but not the adenosine receptor. *J Neurosci* 2009;29:11029–37.
35 Haskó G, Cronstein B. Methylxanthines and inflammatory cells. *Handb Exp Pharmacol* 2011;(200):457–68.

36 Perides G, Laukkarinen JM, Vassileva G, *et al*. Biliary acute pancreatitis in mice is mediated by the G-protein-coupled cell surface bile acid receptor Gpbar1. *Gastroenterology* 2010;138:715–25.
37 Camello PJ, Petersen OH, Toescu EC. Simultaneous presence of cAMP and cGMP exert a co-ordinated inhibitory effect on the agonist-evoked Ca2+ signal in pancreatic acinar cells. *Pflugers Arch* 1996;432:775–81.
38 Echeverri D, Montes FR, Cabrera M, *et al*. Caffeine's vascular mechanisms of action. *Int J Vasc Med* 2010;2010:834060.
39 Bonati M, Latini R, Tognoni G, *et al*. Interspecies comparison of in vivo caffeine pharmacokinetics in man, monkey, rabbit, rat, and mouse. *Drug Metab Rev* 1984–1985;15:1355–83.
40 Hirose K, Iino M, Endo M. Caffeine inhibits Ca(2+)-mediated potentiation of inositol 1,4,5-trisphosphate-induced Ca2+ release in permeabilized vascular smooth muscle cells. *Biochem Biophys Res Commun* 1993;194:726–32.
41 Akin BL, Hurley TD, Chen Z, *et al*. The structural basis for phospholamban inhibition of the calcium pump in sarcoplasmic reticulum. *J Biol Chem* 2013;288:30181–91.
42 Smani T, Shapovalov G, Skryma R, *et al*. Functional and physiopathological implications of TRP channels. *Biochim Biophys Acta* 2015;1853:1772–82.
43 Vigna SR, Shahid RA, Liddle RA. Ethanol contributes to neurogenic pancreatitis by activation of TRPV1. *FASEB J* 2014;28:891–6.
44 Schwartz ES, Christianson JA, Chen X, *et al*. Synergistic role of TRPV1 and TRPA1 in pancreatic pain and inflammation. *Gastroenterology* 2011;140:1283–91.
45 Orabi AI, Shah AU, Ahmad MU, *et al*. Dantrolene mitigates caerulein-induced pancreatitis in vivo in mice. *Am J Physiol Gastrointest Liver Physiol* 2010;299:G196–204.
46 Husain SZ, Orabi AI, Muili KA, *et al*. Ryanodine receptors contribute to bile acid-induced pathological calcium signaling and pancreatitis in mice. *Am J Physiol Gastrointest Liver Physiol* 2012;302:G1423–33.
47 Gerasimenko JV, Maruyama Y, Yano K, *et al*. NAADP mobilizes Ca2+ from a thapsigargin-sensitive store in the nuclear envelope by activating ryanodine receptors. *J Cell Biol* 2003;163:271–82.
48 Burnstock G, Novak I. Purinergic signalling in the pancreas in health and disease. *J Endocrinol* 2012;213:123–41.
49 Satoh A, Shimosegawa T, Satoh K, *et al*. Activation of adenosine A1-receptor pathway induces edema formation in the pancreas of rats. *Gastroenterology* 2000;119:829–36.
50 Noji T, Nan-ya K, Katagiri C, *et al*. Adenosine uptake inhibition ameliorates cerulein-induced acute pancreatitis in mice. *Pancreas* 2002;25:387–92.
51 Barletta KE, Ley K, Mehrad B. Regulation of neutrophil function by adenosine. *Arterioscler Thromb Vasc Biol* 2012;32:856–64.
52 Conlay LA, Conant JA, deBros F, *et al*. Caffeine alters plasma adenosine levels. *Nature* 1997;389:136.

SUPPLEMENTARY MATERIALS AND METHODS

Isolation of pancreatic acinar cells

Pancreatic acinar cells were freshly isolated from pancreata of young adult CD1 mice (8-12 week old) using a standard collagenase (Worthington Biochemical Corporation, Lakewood, NJ, USA) digestion procedure established in previous work.[6-10 S1] All experiments were performed at room temperature (23-25°C) unless otherwise indicated and cells were used within 4 h of isolation. The extracellular solution contained (mM): 140 NaCl, 4.7 KCl, 1.13 $MgCl_2$, 1 $CaCl_2$, 10 D-glucose, 10 HEPES. The final pH of the solution was adjusted to pH 7.35 using NaOH. For experiments longer than two hours, a modified solution was used. The standard physiological saline solution was supplemented with 1X minimal essential amino acid solution, 292 µg ml^{-1} L-glutamine, 100 µg ml^{-1} penicillin and streptomycin, 1 mg ml^{-1} soybean trypsin inhibitor, 1 mM $Na_3PO_4 \cdot 12H_2O$ and 1 mM pyruvate. The solution was sterilised by passing it once through a 200 nm filter (Appleton Woods, Selly Oak, UK).

Caffeine dose optimisation and other methylxanthine administration *in vivo*

To determine the optimal protocol of caffeine injections, we performed several preliminary experiments. We administered 100 mg/kg caffeine (7 intraperitoneal (i.p.) injections at hourly intervals), aiming to achieve a serum concentration of 5 mM, previously shown to inhibit toxin-induced elevations of the acinar cell cytosolic Ca^{2+} concentration ($[Ca^{2+}]_c$).[10, 23, 27 S2] Mice died at this dose, so the dose was reduced to 50 mg/kg, using the same injection protocol. At this dose mice survived but resulted in caffeine intoxication syndrome with irritability, increased urination and muscle twitching. The dose was reduced further to 25 mg/kg using the same protocol. At this

dose no neuro-excitotoxicity was observed. However, in the fatty acid ethyl ester-induced acute pancreatitis, 7 injections of 25 mg/kg caffeine (25 mg/kg regimen) resulted in several mouse fatalities so the injections were reduced to two injections, with the second of these one h after the first. 25 mg/kg theophylline or paraxanthine (7 i.p. injections at hourly intervals) resulted in no discernible side effects.

Serum sampling protocol for di- and trimethylxanthine assay in CER-AP

The 25 mg/kg caffeine regimen was given by injection at the same time as caerulein injections from the third caerulein injection in CER-AP, with two further caffeine injections at hourly intervals after the seventh caerulein injection. Serum samples were taken prior to the first caffeine injection, 10 min after the fourth caffeine injection and 10 min after the seventh caffeine injection as well as two and six hours after the seventh caffeine injection. Serum samples were then assayed by LC/MS for di- and trimethylxanthines. The same administration and sampling protocols were used to assay serum samples before and after theophylline or paraxanthine administration in CER-AP.

Serum amylase and serum IL-6 levels

Serum amylase was tested using a kinetic method by Roche automated clinical chemistry analyzers (GMI, Leeds, UK). Serum IL-6 levels were measured by the ELISA method using the protocols provided by R&D Systems (Abingdon, UK).

Pancreatic oedema

Pancreatic oedema was assessed by measuring pancreatic water content. A portion of pancreas (~60 mg) taken at the time of AP severity assessment was sliced, then

weighed and incubated at 90°C for 72 h. The fully dried tissue was weighed again and the pancreatic water content calculated as: wet weight-dry weight/wet weight ×100%.

Pancreatic trypsin activity

Pancreata were homogenised by a motorised homogeniser on ice in tissue buffer pH 6.5, containing (in mM) MOPS 5, sucrose 250 and magnesium sulfate 1. The homogenates were centrifuged at 1500 g for 5 min, and 100 µl of each supernatant was added to a cuvette containing the peptide substrate Boc-Gln-Ala-Arg-MCA (Peptide, Osaka, Japan) dissolved in 1900 µl pH 8.0 assay buffer containing (in mM) Tris 50, NaCl 150, $CaCl_2$ 1 and 0.1 mg/mL bovine serum albumin. Trypsin activity was measured by fluorimetric assay using a Shimadzu RF-5000 spectrophotometer (Milton Keynes, UK). Samples were excited at 380 nm and emissions collected at 440 nm[S2 S3]. A standard curve was generated using purified human trypsin. Pancreatic protein concentration was measured by a BCA protein assay (Thermo, Rockford, USA) using a BMG FlUOstar Omega Microplate Reader (Imgen Technologies, New York, USA). Trypsin activity was expressed as fmol/mg protein.

Myeloperoxidase activity

Myeloperoxidase activity in pancreas and lung was tested by a modified method from Dawra et al[S4]. Myeloperoxidase activity was measured by using the substrate 3,3′,5,5′-tetramethylbenzidine (TMB) in extracted supernatants from the samples. Briefly, 20 µl of the supernatant was added into the assay mix which consisted of 200 µL of phosphate buffer (100 mM, pH 5.4) with 0.5% HETAB and 20 µl TMB (20 mM in DMSO). This mixture was incubated at 37°C for 3 min, followed by addition of

50 µL H_2O_2 (0.01%). The mixture was further incubated for 3 min. The difference of absorbance between 0 min and 3 min at 655 nm was calculated against a standard curve generated by human myeloperoxidase using a plate reader.

Histopathology

Pancreatic and lung tissues were subjected to H&E staining and cut into 5 µm slides. For all experimental groups, 10 random fields of each pancreatic slide were graded by two independent blinded observers at magnification x200. Severity of pancreatic injury was defined by the extent of edema, inflammatory cell infiltration and acinar necrosis as previously described (each was scored as 0-3), and overall histopathology score calculated as the sum of individual scores.[10, 15] Lung histolopathology scores were determined by two independent blinded observers grading alveolar septal thickening in 10 random fields of each lung slide at magnification x200 (scored as 0-3 where 0 = normal, 1 = thickening <1/3 field, 2 = thickening ≥1/3 field and ≤ 2/3 field and 3 = thickening >2/3 field).

Measurement of pancreatic blood flow by fluorescent microsphere

To measure pancreatic blood flow, mice received either intraperitoneal injections of 50 µg/kg caerulein (CER, 7 injections hourly) or an equal number of equivalent volume saline injections. CAF (25 mg/kg) was given simultaneously with each CER injection. Mice were humanely killed 1 h after the last CER/CAF injection. The method to measure flow was adapted from that published by the Fluorescent Microsphere Resource Centre in the University of Washington (http://fmrc.pulmcc.washington.edu).[S5] In brief, male CD1 mice (35 g) had general anaesthesia induced and maintained with isofluorane. Under a dissecting

microscope, the left common carotid artery was accessed, ligated cranially and cannulated using 0.6 mm diameter polyethylene tubing. The tubing was advanced just beyond the thoracic inlet and secured using a bulldog clip. 200 IU of unfractionated sodium heparin was injected, followed by slow bolus injection of 0.5 ml phosphate buffered saline containing 140,000 red 10 μm diameter polystyrene microbeads (FluoSpheres, Red (580/605), Molecular Probes Europe, Leiden, The Netherlands) over 60 seconds. Animals were culled by intravascular injection of pentobarbital and organs (pancreas, lung, kidneys) harvested immediately. Whole organs were placed in 1.5 ml Eppendorf tubes and weighed prior to further processing.

36,000 blue-green polystyrene microspheres (430/465) were added to each Eppendorf tube as procedural controls and organs digested in 1 ml of ethanolic KOH for 48h at 50 °C, vortexing at 24 and 48 h. Tubes were then centrifuged at 2000 g for 20 min and pellets resuspended in distilled water with 1% Triton-100, vortexed and again centrifuged at 2000 g for 20min. Pellets were resuspended in phosphate buffer (pH 7), vortexed and centrifuged before resuspending in 1ml of 2-ethoxy-ethyl acetate, vortexed and kept in a dark at room temperature for 24 h. Samples were then centrifuged at 2000 g for 20min and fluorescence of supernatants determined using the BMG FlUOstar Omega Microplate Reader (BMG LABTECH, Aylesbury, UK), sequentially measuring red (420/460) and blue-green fluorescence (580/620).

Individual experimental results were excluded if blue-green fluorescence differed by >20% from average, indicating loss of spheres during processing. Results were also excluded if the difference in red fluorescence between left and right kidneys was

>20%, indicating inadequate mixing of spheres prior to injection. Fluorescent values per weight of pancreas were compared between experimental groups, with n ≥ 4 experimental repeats per group.

SUPPLEMENTARY FIGURE LEGENDS

Supplementary Figure 1. Effect of monomethylxanthine and xanthine on ACh-induced Ca^{2+} oscillations in isolated pancreatic acinar cells. **(A)** 1-methylxanthine (1-MX, 2 mM) had minimal inhibitory effect on ACh-induced Ca^{2+} oscillations, while **(B)** Xanthine (2 mM) did not show any effect. Traces are averages from >20 cells from at least three repeat experiments. Data are normalised from basal fluorescence levels (F/F_0).

Supplementary Figure 2. Effect of caffeine (CAF) on CCK- and TLCS-induced Ca^{2+} plateaus in isolated pancreatic acinar cells. **(A)** CAF (10 mM) nearly abolished CCK-induced Ca^{2+} plateaus. (B) CAF (10 mM) converted TLCS-induced Ca^{2+} plateaus into oscillations. Traces are averages from >20 cells from at least three repeat experiments. Data are normalised from basal fluorescence levels (F/F_0).

Supplementary Figure 3. Phosphodiesterase inhibitors block ACh-induced Ca^{2+} oscillations in isolated pancreatic acinar cells. **(A)** Non-selective phosphodiesterase inhibitors methylxanthines (MXs) - caffeine (CAF), theophylline (TP), paraxanthine (PX), theobromine (TB), 1-MX, 7-MX and 3-isobutyl-1-methylxanthine (IBMX) showed significant dose-dependent inhibition at 500 µM and 2 mM. TP (2 mM) showed the greatest inhibition that was similar to the IBMX positive control. Mono-MXs showed the least inhibition, and no significant inhibition was detected with 500

μM 7-MX (*p <0.05 vs control; †p <0.05 vs lower concentration). **(B)** IBMX (2 mM) and **(C)** a synthesised MX derivative pentoxfylline (PTX, 2 mM) were shown to have a complete inhibitory effect on ACh-induced Ca^{2+} oscillations. **(D)** (i) No significant inhibitory effect was observed when rolipram (ROL), a selective non-xanthine based phosphodiesterase 4 inhibitor, at 100 μM was used. (ii) A marked inhibition, however, was achieved when the concentration of ROL was increased to 200 μM. Traces are averages of >20 cells from at least three repeat experiments. Data are normalised from basal fluorescence levels (F/F_0) and expressed as means ± SE in histograms.

Supplementary Figure 4. Effects of caffeine (CAF) on lung histopathology, renal function, renal histology and pancreatic blood flow in CER-AP. **(A)** Representative images of lung histopathology for in controls, CER-AP and CER-AP with caffeine (H&E, ×200) and **(C)** lung histopathology scores. **(D)** Serum creatinine and **(E)** representative images of kidney histology for all groups and caffeine alone (H&E, ×200). (E) Pancreatic blood flow in all three groups. (*p <0.05 vs other groups. Values are means ± SE of 4-6 animals per group).

Supplementary Figure 5. Dose response of dimethylxanthines on the severity of CER-AP at 12 h. Mice received intraperitoneal injections of 50 μg/kg caerulein (7 injections hourly) and either theophylline (TP) or paraxanthine (PX) at either 10 and 25 mg/kg regimens (7 injections hourly) was given 2 h after the first injection of caerulein. Control groups received the same volume of saline injections from 2 h after the first injection of caerulein. Mice were humanely killed at 12 h after disease induction and assessed by **(A)** Serum amylase, **(B)** Pancreatic oedema, **(C)**

Pancreatic trypsin activity and **(D)** Pancreatic myeloperoxidase (MPO) activity (normalised to saline group). **(E)** (i) Overall histopathological score and breakdown of components: (ii) oedema, (iii) inflammation and (iv) necrosis. *$p<0.05$ vs saline group. Values are means ± SE of 6 animals per group.

Supplementary Figure 6. Determination of dimethylxanthine levels in CER-AP. Mice received either intraperitoneal injections of 50 µg/kg caerulein (7 injections hourly). Theophylline (TP) or paraxanthine (PX) at either 10 or 25 mg/kg regimen (7 injections hourly) was given respectively 2 h after the first injection of caerulein. Mice were humanely killed at 12 h after disease induction and serum dimethylxanthine levels assessed by LC/MS. **(A)** Serum mean levels of TP were 18.1 and 67.4 µM for 10 and 25 mg/kg TP regimens, respectively. **(B)** Mean serum levels of PX were 48.0 and 91.0 µM for 10 and 25 mg/kg PX regimens, respectively. Values are means ± SE of 6 animals per group.

SUPPLEMENTARY REFERENCES

S1. Booth DM, Murphy JA, Mukherjee R, *et al.* Reactive oxygen species induced by bile acid induce apoptosis and protect against necrosis in pancreatic acinar cells. *Gastroenterology* 2011;140:2116-25.

S2. Nathan JD, Romac J, Peng RY, *et al.* Transgenic expression of pancreatic secretory trypsin inhibitor-I ameliorates secretagogue-induced pancreatitis in mice. *Gastroenterology* 2005;128:717-27.

S3. Kawabata S, Miura T, Morita T, *et al.* Highly sensitive peptide-4-methylcoumaryl-7-amide substrates for blood-clotting proteases and trypsin. *FEBS J* 1988;172:17-25.

S4. Dawra R, Ku YS, Sharif R, *et al.* An improved method for extracting myeloperoxidase and determining its activity in the pancreas and lungs during pancreatitis. *Pancreas* 2008;37:62-8.

S5. Manual for using fluorescent microspheres to measure regional organ perfusion. Seattle, WA: University of Washington, 1999.

Figure S1

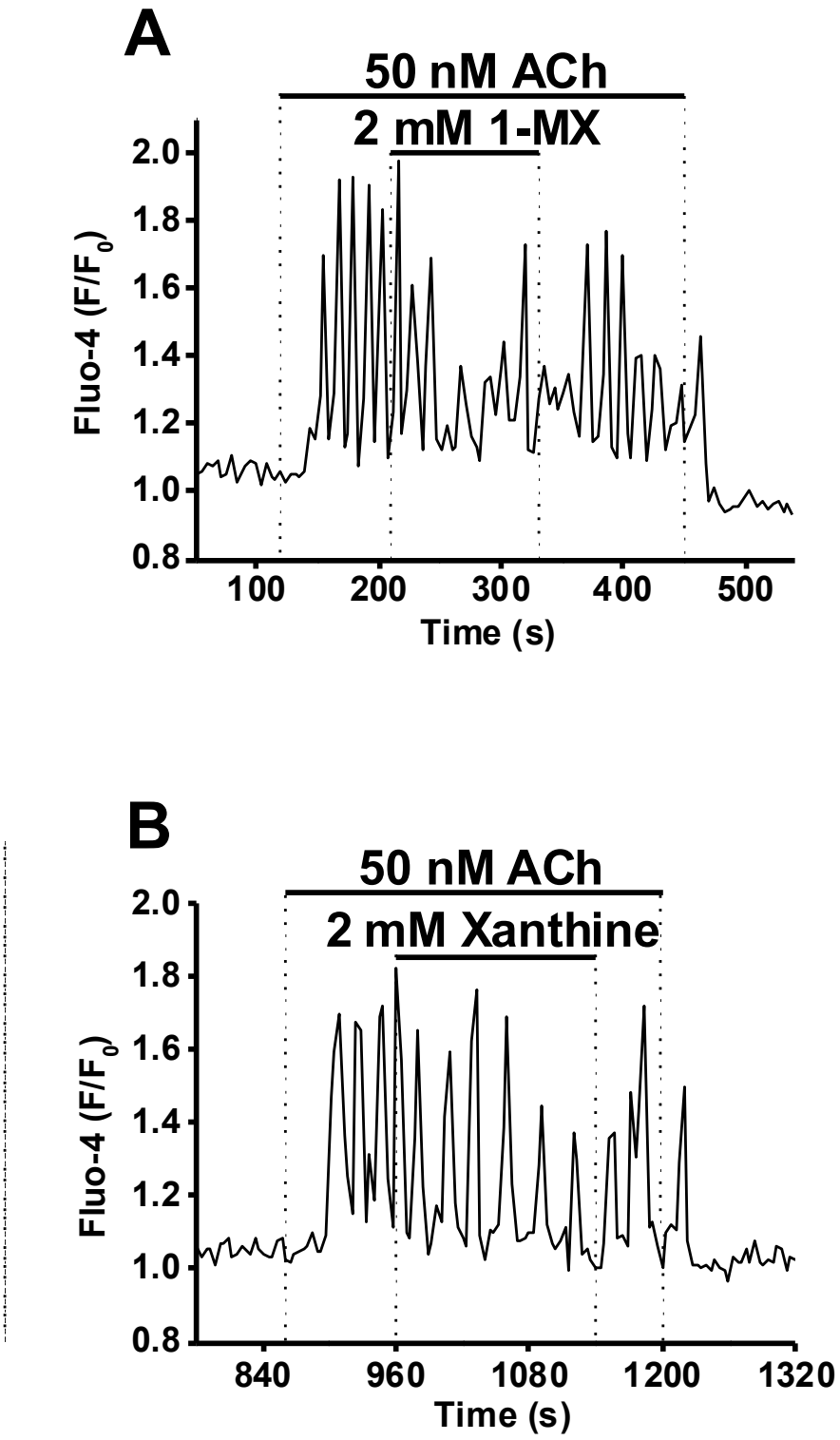
A
50 nM ACh
2 mM 1-MX
Fluo-4 (F/F0)
2.0
1.8
1.6
1.4
1.2
1.0
0.8
100
200
300
400
500
Time (s)
B
50 nM ACh
2 mM Xanthine
Fluo-4 (F/F0)
2.0
1.8
1.6
1.4
1.2
1.0
0.8
840
960
1080
1200
1320
Time (s)

Figure S2

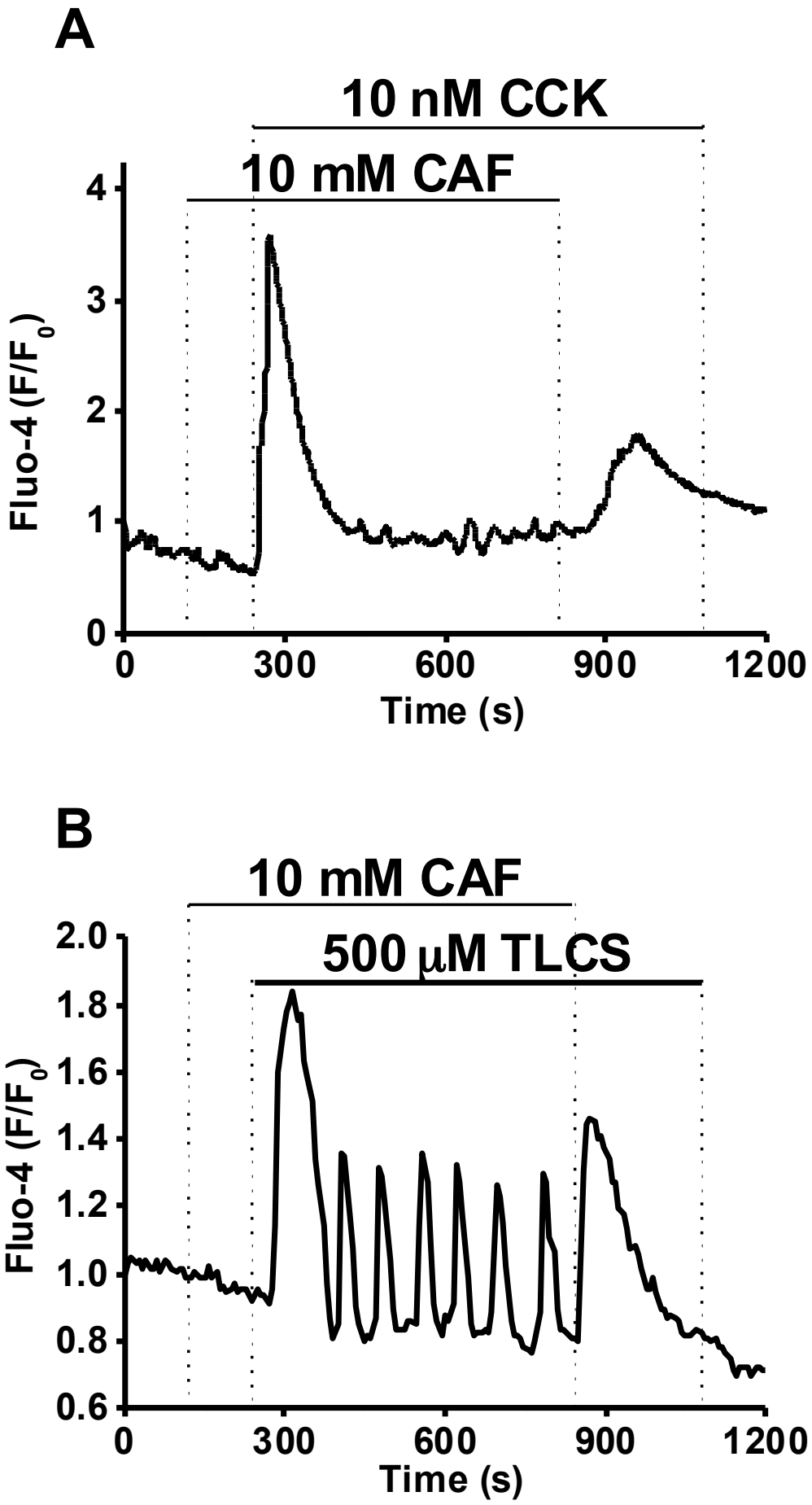
A
10 nM CCK
10 mM CAF
Fluo-4 (F/F0)
0
1
2
3
4
0
300
600
900
1200
Time (s)
B
10 mM CAF
500 μM TLCS
Fluo-4 (F/F0)
0.6
0.8
1.0
1.2
1.4
1.6
1.8
2.0
0
300
600
900
1200
Time (s)

Figure S3

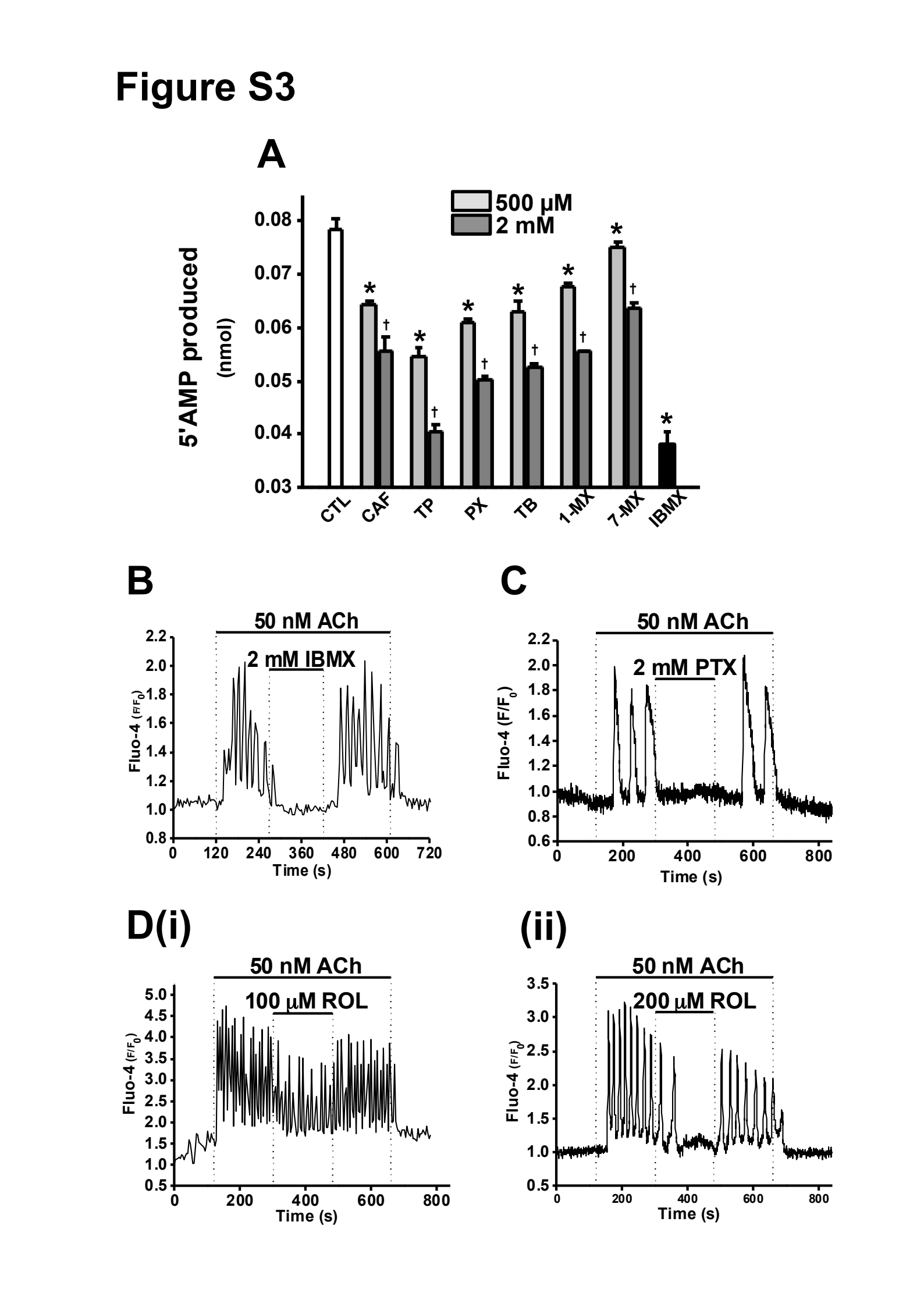
A
500 µM
2 mM
5'AMP produced
(nmol)
0.08
0.07
0.06
0.05
0.04
0.03
CTL
CAF
TP
PX
TB
1-MX
7-MX
IBMX
B
50 nM ACh
2 mM IBMX
Fluo-4 (F/F0)
Time (s)
C
50 nM ACh
2 mM PTX
Fluo-4 (F/F0)
Time (s)
D(i)
50 nM ACh
100 µM ROL
Fluo-4 (F/F0)
Time (s)
(ii)
50 nM ACh
200 µM ROL
Fluo-4 (F/F0)
Time (s)

Figure S4

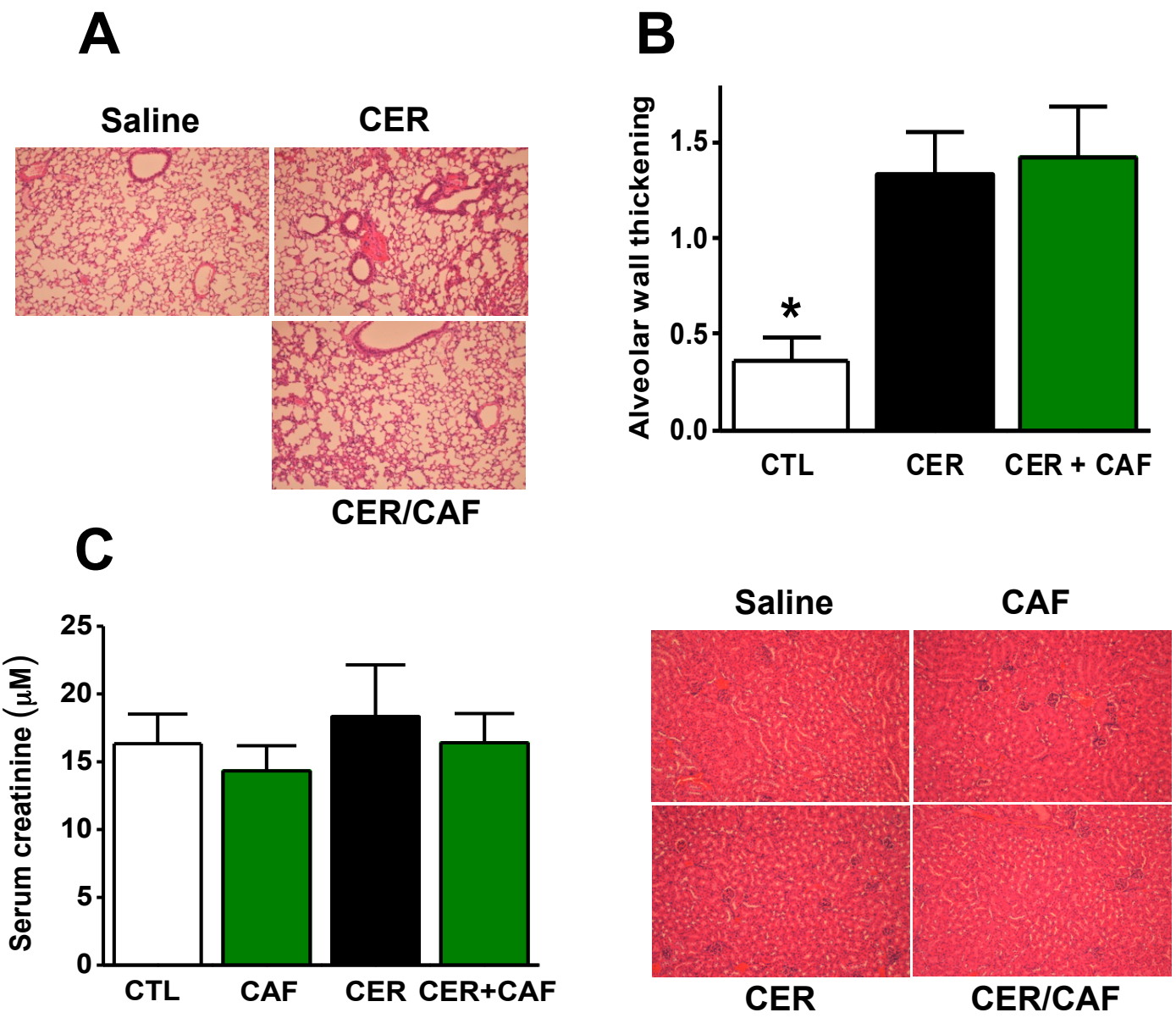
A
Saline
CER
CER/CAF
B
Alveolar wall thickening
1.5
1.0
0.5
0.0
*
CTL
CER
CER + CAF
C
Serum creatinine (μM)
25
20
15
10
5
0
CTL
CAF
CER
CER+CAF
Saline
CAF
CER
CER/CAF
C
Fluorescence/g weight
100
80
60
40
20
0
*
CTL
CER
CER + CAF

Figure S5

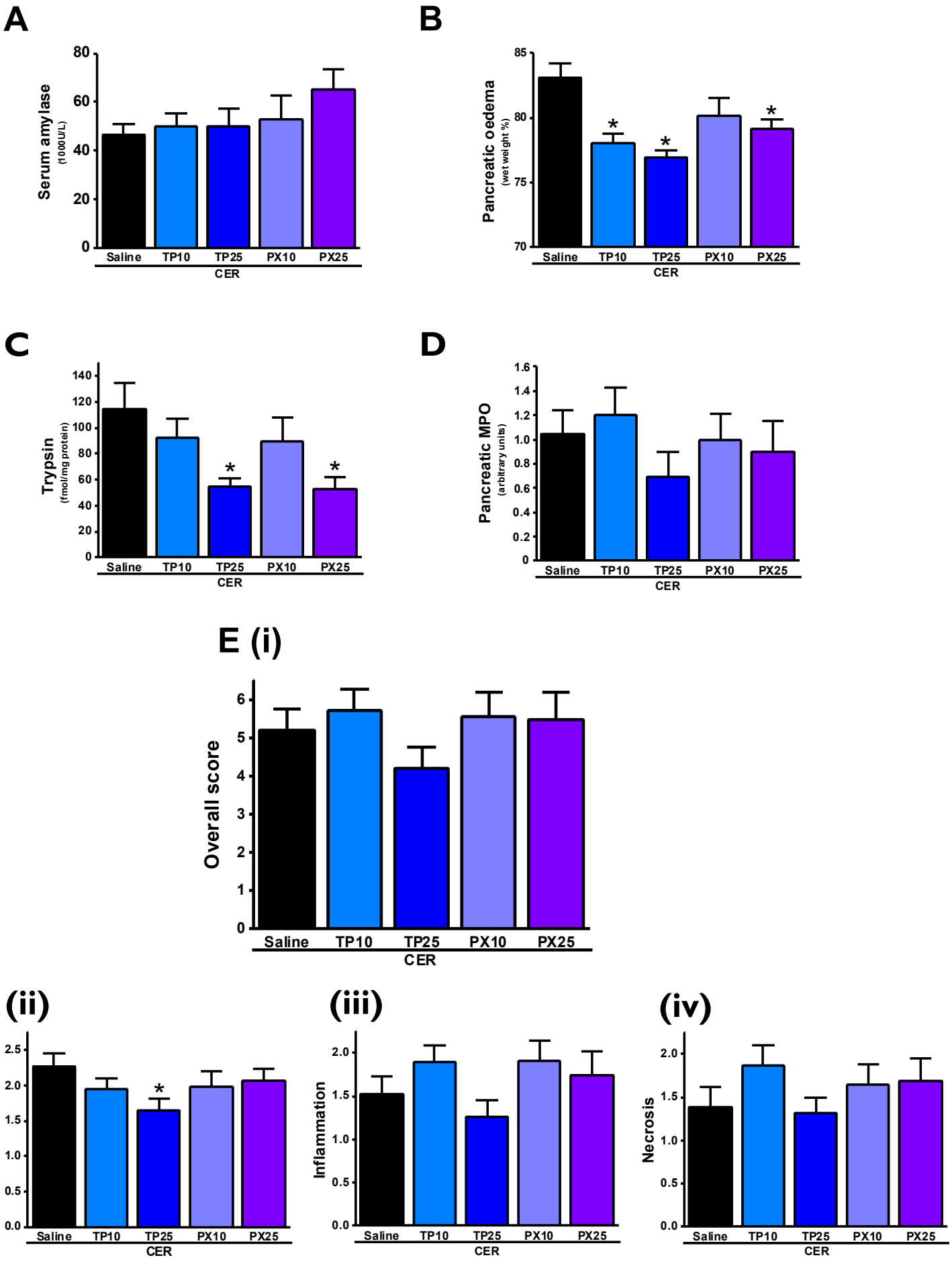
A
Serum amylase
(1000U/L)
80
60
40
20
0
Saline
TP10
TP25
PX10
PX25
CER
B
Pancreatic oedema
(wet weight %)
85
80
75
70
*
*
*
Saline
TP10
TP25
PX10
PX25
CER
C
Trypsin
(fmol/mg protein)
140
120
100
80
60
40
20
0
*
*
Saline
TP10
TP25
PX10
PX25
CER
D
Pancreatic MPO
(arbitrary units)
1.6
1.4
1.2
1.0
0.8
0.6
0.4
0.2
0
Saline
TP10
TP25
PX10
PX25
CER
E (i)
Overall score
6
5
4
3
2
1
0
Saline
TP10
TP25
PX10
PX25
CER
(ii)
Oedema
2.5
2.0
1.5
1.0
0.5
0.0
*
Saline
TP10
TP25
PX10
PX25
CER
(iii)
Inflammation
2.0
1.5
1.0
0.5
0.0
Saline
TP10
TP25
PX10
PX25
CER
(iv)
Necrosis
2.0
1.5
1.0
0.5
0.0
Saline
TP10
TP25
PX10
PX25
CER

Figure S6